ISSN 2631-4843

The British Astronomical Association

Variable Star Section Circular

No. 201 September 2024

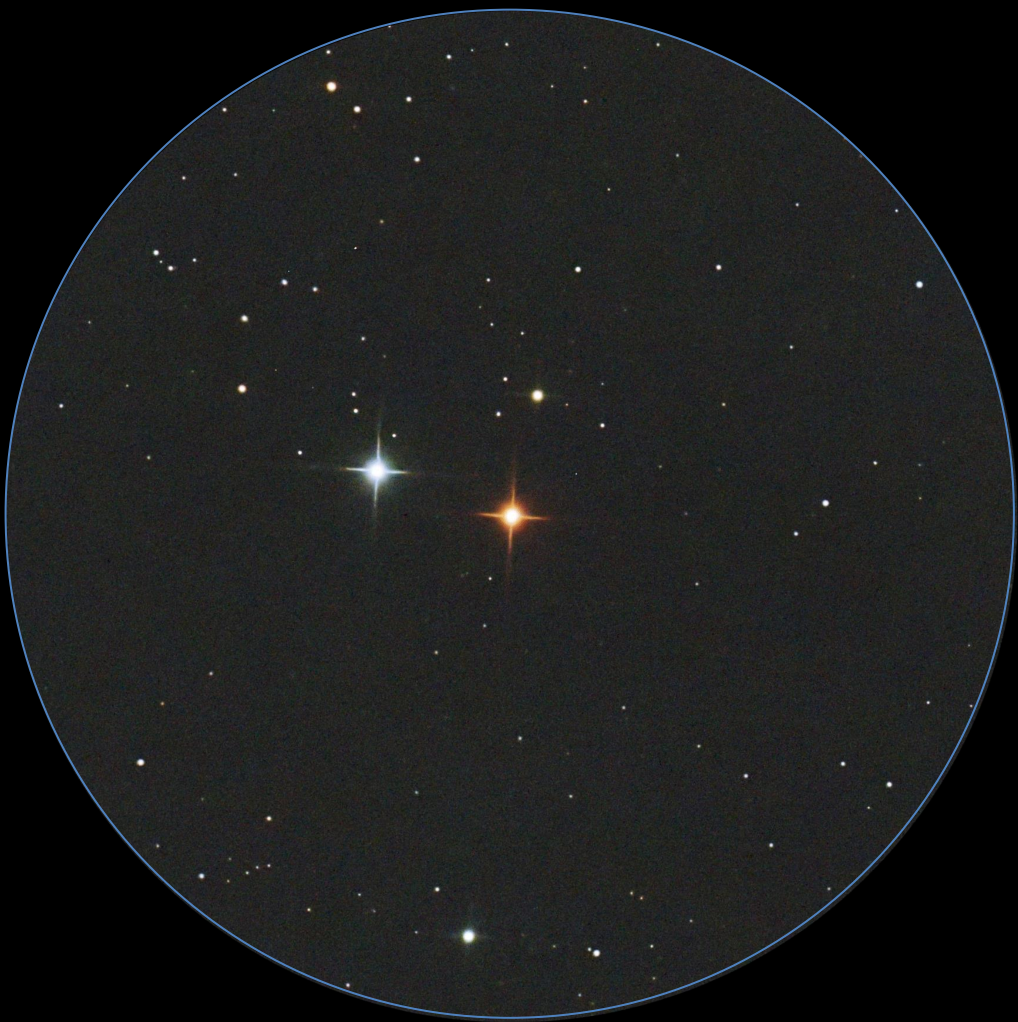

BAA Office: PO Box 702, Tonbridge TN9 9TX

Contents

Cover Picture

The Semi-Regular Variable π1 Grus (type SRB 5.3-7.0V)

Mazin Younis

From the Director – *Jeremy Shears*

Welcome to the 201st edition of the VSS Circular. It was wonderful to hear the favourable response following the publication of the 200th edition in June.

September 1st marks my fifth anniversary as Director. Where did those five years go? I am grateful for the support that I have received from section members and the VSS Officers during this time. And a big thank all to our observers who go out night after night, whatever the weather, to monitor the variable stars.

In my mind at least, the new observing season begins on September 1st. In anticipation, I have repainted the outside of my observatory dome and cleaned inside. The presence of spiders and cobwebs I can understand, but I am still trying to work out where all those desiccated slugs come from! During August my CCD camera failed. After 15 years of use, it owed me precisely nothing. It has now been replaced by a Starlight Xpress Trius Pro 694, which I am glad to say, worked flawlessly straight out of the box. Let's hope for some clear autumn nights ahead.

Nova Vulpeculae 2024 (V615 Vul)

Whilst the world awaits the next eruption of T CrB (we are still within the February to September window of Prof. Brad Schaefer's most recent prediction for the eruption), this summer we were treated to another nova. Nova Vulpeculae 2024 was discovered on July 29.832 UT at an unfiltered CCD magnitude of 11.2 by the New Milky Way Survey and reported on behalf of the survey team by K. Sokolovsky (University of Illinois and Sternberg Astronomical Institute). It's not often we get to enjoy a reasonably bright northern nova, especially one so conveniently positioned in the evening sky. The nova, which reached magnitude 9.6 has been followed by our observers visually, electronically and spectroscopically. It has the official name of V615 Vul.

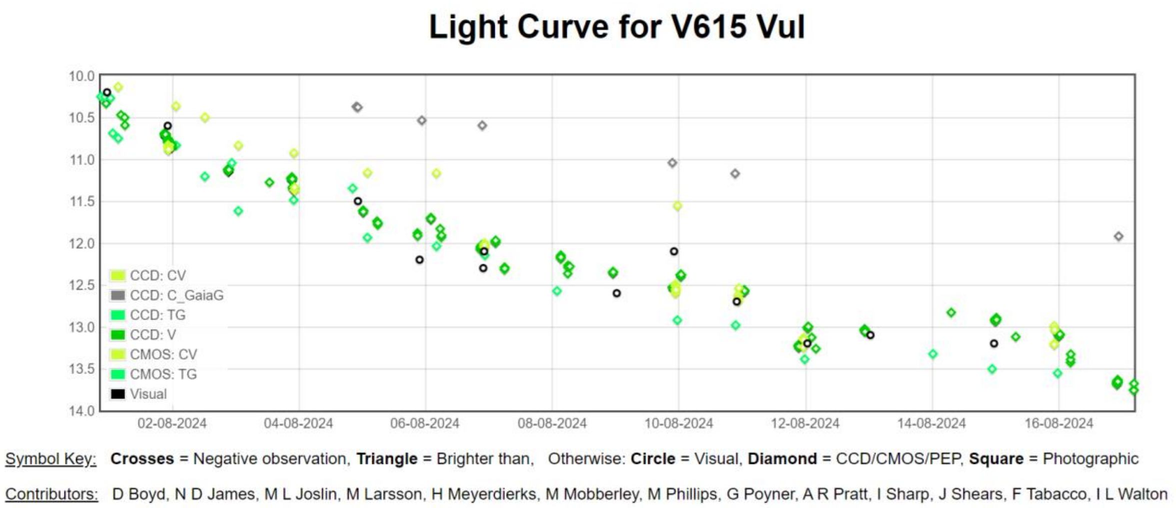

Smart telescopes

It is extraordinary to see the increasing popularity of smart telescopes, such as the Vaonis Vespera, Unistellar eVscope, Dwarflab Dwarf II and ZWO Seestar S50. These instruments are producing some really impressive images. The next step is to see them contributing to scientific projects. Several observers are routinely imaging the field of T CrB to see if they can detect the eruption.

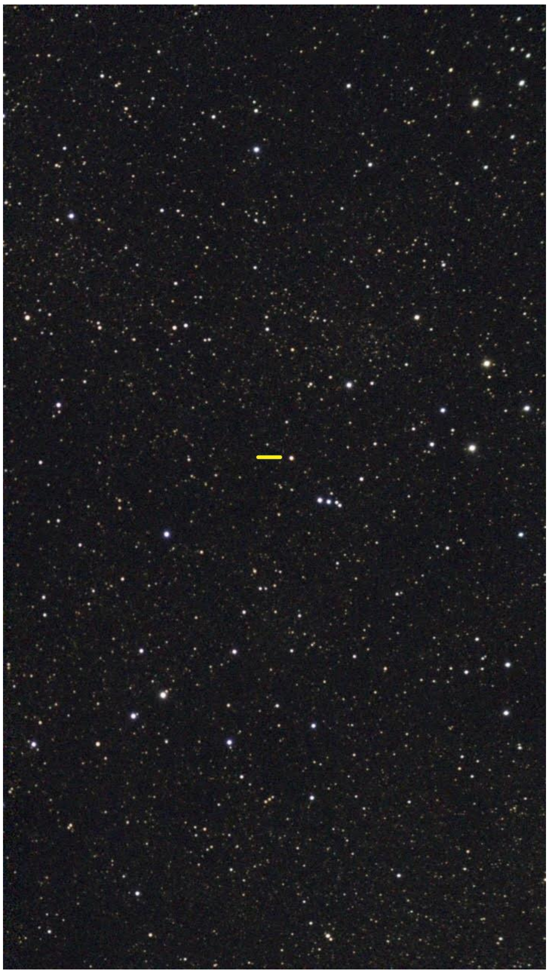

Despite their small aperture, smart telescopes are clearly very capable astrographs presented in a compact and user-friendly package. It will be interesting to see what sort of photometry these instruments are able to yield (if anyone has tackled extracting accurate photometry with one of these devices, perhaps you could write about in in a future Circular). I also wonder whether they might have a role to play in nova patrolling. Given the effectiveness of widefield camera lenses coupled to digital cameras in detecting novae, like V615 Vul, perhaps it won't be too long before we see a consumer smart telescope achieving similar success.

V615 Vul imaged with a ZWO Seestar S50 on 2024 Aug 1, 15 min exposure, 0°42′ × 1°15′ (Mark Hardaker, Verwood, Dorset)

Michael Woodman and his independent discovery of T CrB in 1946

In VSSC 199 (2024 March, page 22) I wrote about Michael Woodman who, at the age of 15, detected the eruption of T CrB in the early hours of 1946 Feb 9 from his home in Newport, South Wales.

Well, thanks to the sleuthing efforts of Finbarr Connolly (Kilfinane Coshlea Historical Society) and Dr Andrew Holmes, I have been able to speak to Michael Woodman who is now 94. He has described to me how he made the discovery and his correspondence with the Astronomer Royal, to whom he reported the discovery. It is wonderful to learn that he continued his interest in astronomy throughout his life. I will write more about this at a later date.

Recent observations of Mira Variables on the BAAVSS programme. 4

Shaun Albrighton

shaunalbrighton93@gmail.com

In this report we examine a further four Mira variables on the BAAVSS programme between January 2016 and July 2024. Of note are the continued reduction in the period of R Hya and error in VSX for range of W Lyn.

R Hya

R Hya is perhaps the most fascinating Mira variable, and yet for observers in northern latitudes, one of the most frustrating. Lying at a declination of -23 degrees means that even from southern Britain, it never rises by more than 17 degrees above the southern horizon. Observers will therefore need a good SE-SW horizon, hopefully relatively free of light pollution. If this were not already a challenge, the star lies south of the ecliptic, so disappears into the Sun's glare during late summer-autumn. For observers in the southern hemisphere the situation is much better, with the star passing near to the zenith. In addition, the star lies higher in the sky than the ecliptic so the period it can be observed is much greater.

VSX [1] lists R Hya as having an extreme range of 3.5 – 10.9V, period 359d, Rise 49% (176d), spectral type M6e-M9e(Tc).

The plot of observations by BAAVSS observers clearly shows the sessional gap in observations and the poor uptake of observers. The second plot is an AAVSO [2] plot between June 2009 and Feb 2023 and includes observations from southern observers. Even so, with a period of currently near to a year meant that for several years the maxima were unobserved.

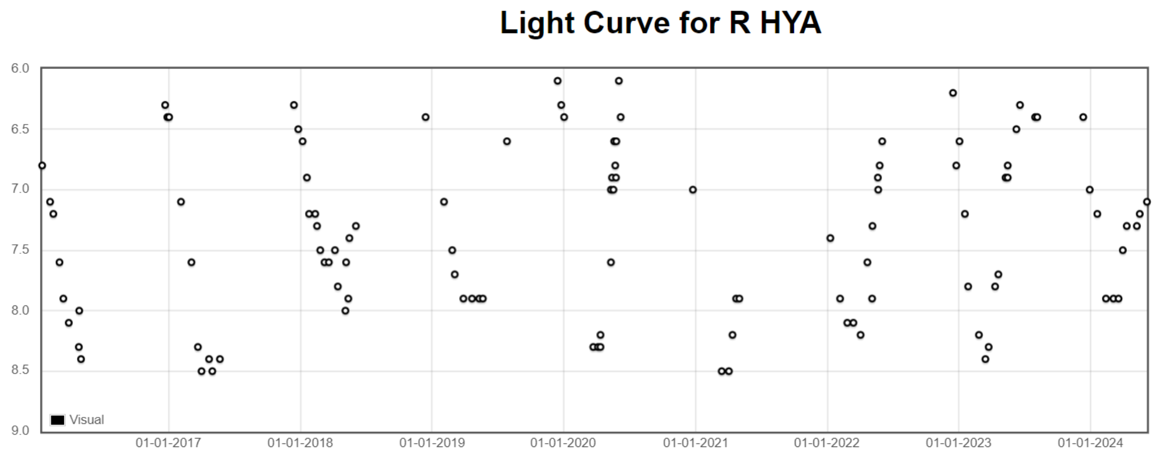

Back to contents

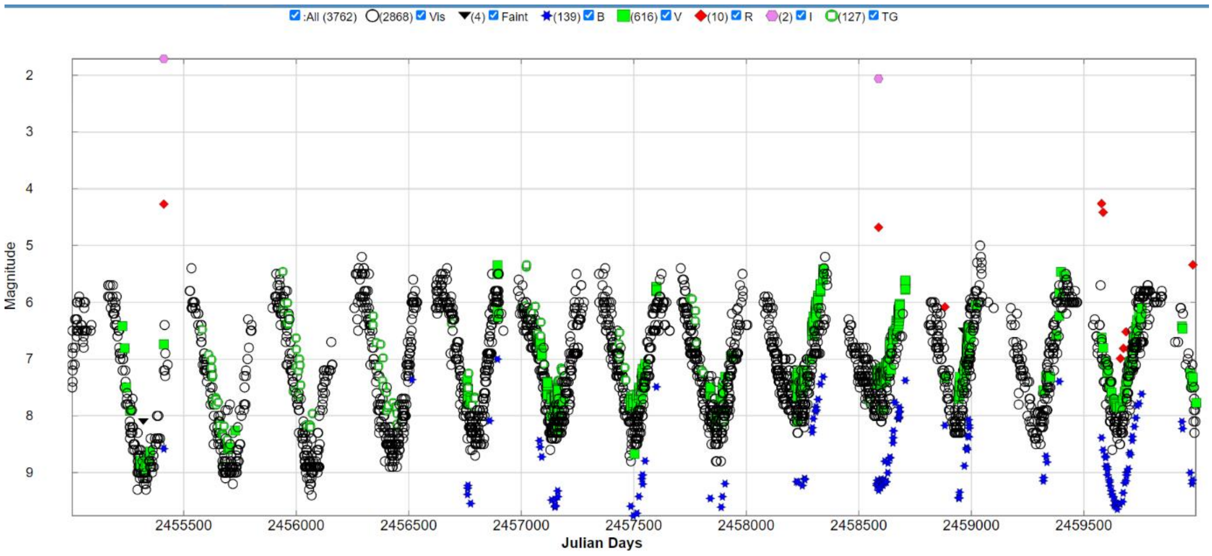

The third plot, again from AAVSO, covers the period 1913-1927. Two things are evident from this plot, firstly that star appears to have experienced brighter maxima and hence a larger range. Secondly, the period has shortened. In fact, if we take a look at how the period has changed over time [3], we see that since 1800, when the period was approximately 490d, it has systematically reduced to currently being 360d

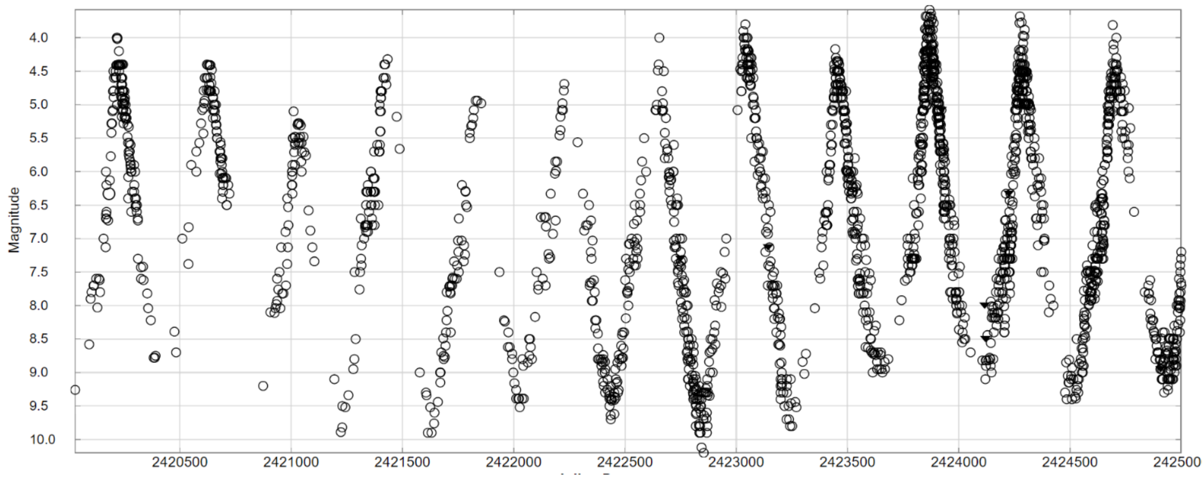

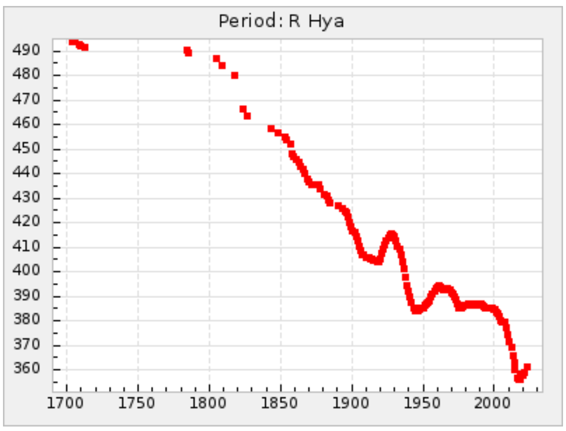

So, is R Hya worth following from the UK? I would answer a big yes. Will the stars period continue to drop, or will it settle down/reverse? Only time will tell.

Back to contents

SU Lac

VSX lists SU Lac as having a range of 11.3-16.0p, period 302d, rise 40% (121d), spectrum M5e.

BAAVSS observation both visually and CCD, indicate maxima between 10.2-11.2, this is to be expected compared to photographic magnitudes. Due to the faintness of the star at minimum the star has not been observed visually at minimum. CCD observations indicate minima of 15.5-16.0V. CCD observers are asked to conduct consistent observations of the star so that meaningful analysis can take place.

Light Curve for SU LAC

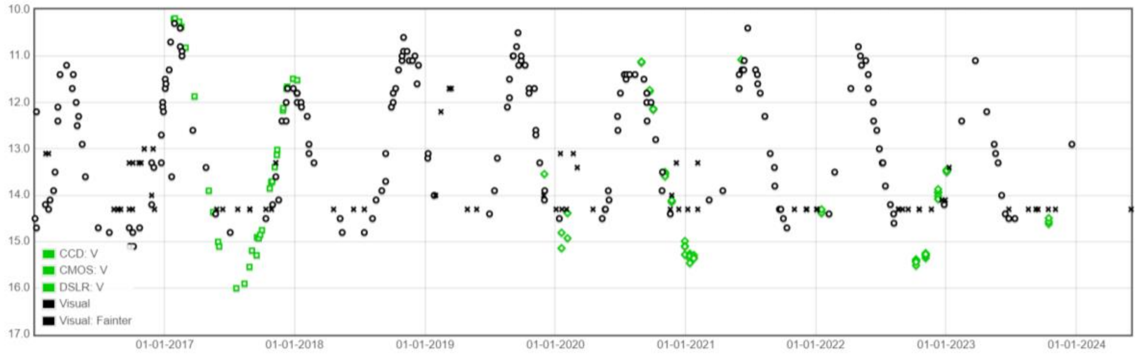

R Leo

VSX lists R Leo as having range 4.4-11.0V, period 312.2d, rise 43% (134d), spectrum M6e-M8IIIe-M9.5e.

Lying near to the ecliptic, R Leo is not observable between early July and mid-September, hence seasonal gaps in the light curve. As can be seen maxima vary between approximately, 5.0 and 6.2, whilst minima have been near to 11.0. R Leo is therefore an ideal target for binoculars or small telescopes. Period analysis shows that the period of the star varies randomly over the range of 306-320d.

Light Curve for R LEO

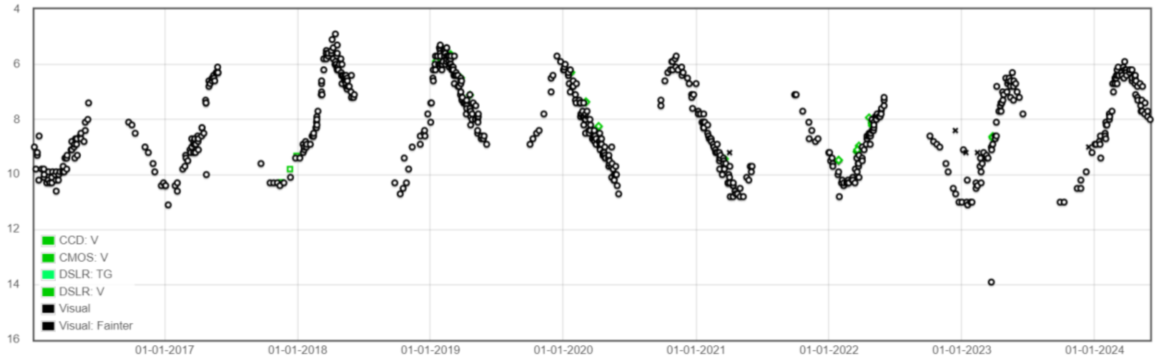

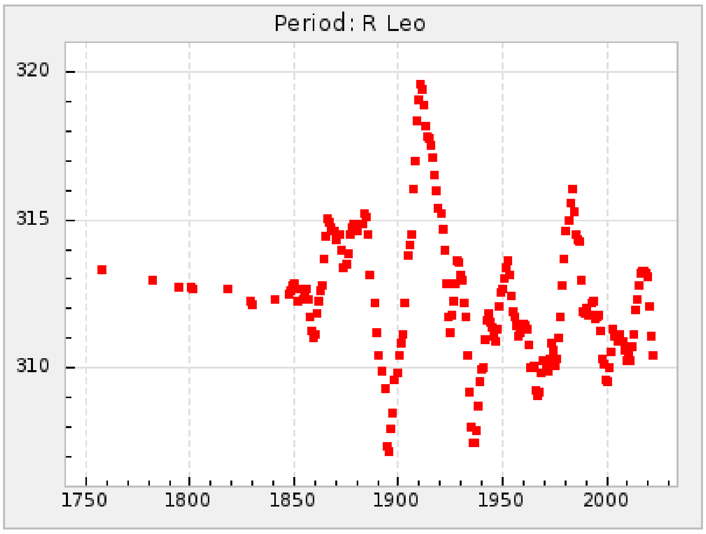

W Lyn

VSX lists W Lyn as having a range of 7.5-14V, period 295.2d, spectrum M6.

Although poorly observed, BAAVSS observations since 2016, show maxima between 9.2 and 10.7, whilst CCD observations indicate that minima are much fainter at 16th magnitude. It would therefore appear that the VSX range is seriously in error, particularly the value of minima. Period analysis shows that the star varies randomly over a small range, 292-297d.

I would ask observers, both visual and CCD, to add this star to their programme, to confirm the range of this star.

Light Curve for W LYN

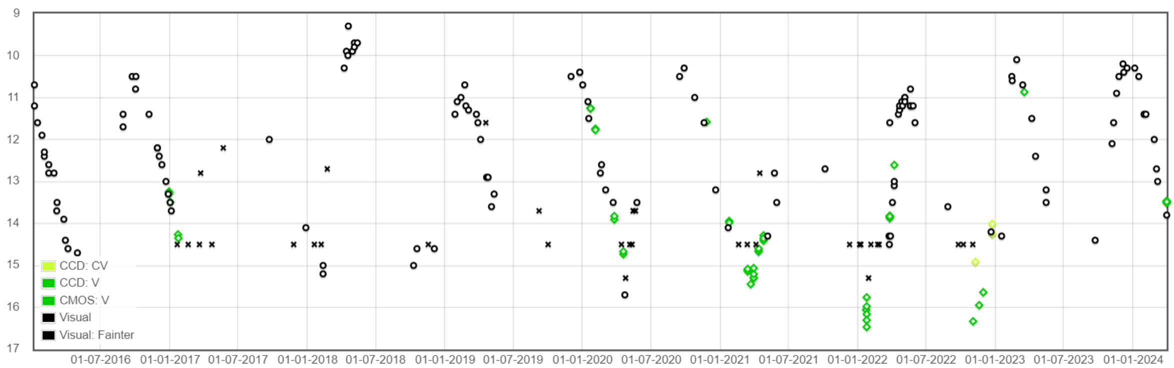

References

1. All data VSX
2. AAVSO
3. Period plots are by Thomas Karlsson (SAF) https://var.saaf.se/mirainfoper.php

Spectroscopic study of short period pulsating stars

Kevin Gurney

kevingurney42@gmail.com

Short period pulsators have peak radial velocities of the order of tens of km/s, and a corresponding Doppler shift of the order of one Angstrom. Obtaining the resulting radial velocity curves challenges the limits of observability with amateur equipment. Here I report observations of two δ-Scuti stars (BE Lyn, SZ Lyn) showing velocity curves in good agreement with published observations.

Overview

Short period pulsating stars owe their intrinsic variability to internal dynamics causing periodic changes in their temperature and radius. The latter is associated with peak radial velocities of the order of tens of km/s, and a corresponding Doppler shift in spectral features of the order of one Angstrom (Å). However, observing the *shape* of the resulting radial velocity curve requires even finer resolution down to at least 0.1Å. This challenges the limits of observability with amateur equipment but, inspired by a BAA talk last year on short period pulsating variables [1], I started a programme of their spectroscopic observation in the Autumn of 2023. Here I report observations of two δ-Scuti stars showing good agreement with published observations.

The targets

Several targets were selected but the two reported here are BE Lyn (8.6 – 9.0V, period 2.3hrs) and SZ Lyn (9.1-9.7V period 2.89hrs). They are both high amplitude δ-Scuti type (HADS) - that is, radial pulsators with light curve amplitudes greater than 0.15 magnitudes [2]. The data for both cover at least one pulsation cycle so that a velocity curve shape can be observed.

General Methods

I used a Shelyak Lhires spectrograph with 2400l/mm grating, a Celestron C11 mounted on a MESU 200, an Atik 460EX as the science camera, and an SX Lodestar2 guide camera. All observations were conducted from Sheffield. Data acquisition was done using Prism [3], and data reduction of spectra was done using my own pipeline written in Python (available on request). Other tools for extracting radial velocities were also written in Python.

During acquisition, calibration frames were frequently taken (typically after every two sub-exposures, automated in Prism) to try and minimise calibration errors due to temperature drift and kit flexure. Spectra were calibrated using the temporally nearest calibration frame.

Results: the spectra

Figure 1 shows a typical spectrum profile from a 300s sub-exposure for BE Lyn†, centred near 4675Å. The profile is rectified, having had any underlying continuum component removed. The 'subs' were grouped together into pairs in the data reduction, giving 10 mins of exposure in total per 1D profile. There are several features here which, while somewhat inconspicuous within the accompanying noise, are reliably reproduced across subs. The prominence of the noise here is not surprising given that magnitudes of 8-9 are at the faint end of observability with this rig.

† All spectra are available from the BAA database

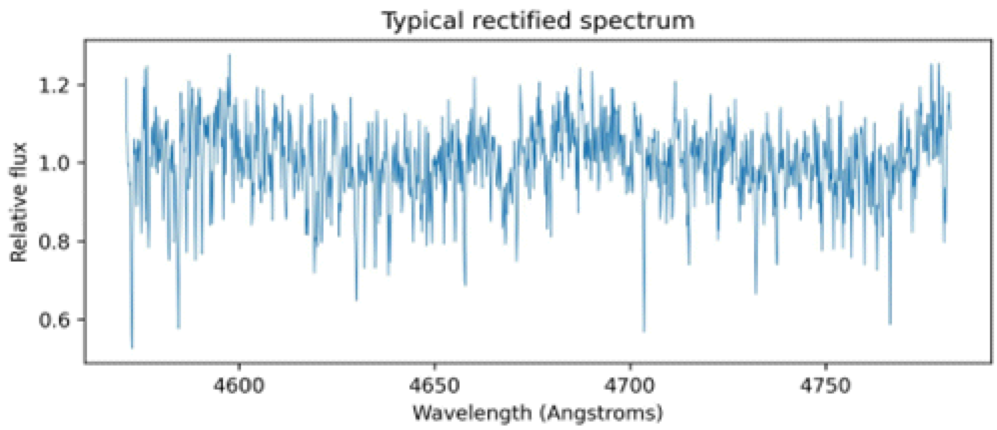

Figure 1. Typical rectified spectral profile of BE Lyn with 300s exposure

Results: seeing pulsation

The radial velocity associated with pulsation is obtained from measuring Doppler shifts in wavelength of spectral features. While a quantitative determination is done with cross-correlation between the spectra, a graphic interpretation is instructive and is shown for BE Lyn in Figure 2.

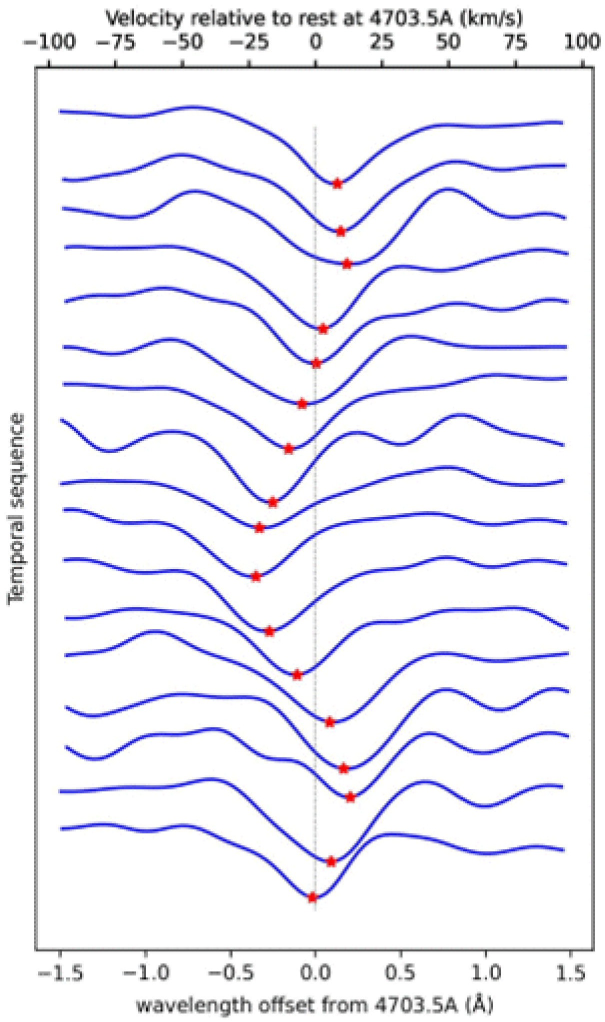

Figure 2: Time series of smoothed spectrum profiles of BE Lyn centred near 4703.5Å. The red symbols show the minimum of the absorption feature.

This shows a wavelength close-up of a series of smoothed spectra taken from a single, 3 hour session, during which there was just over one complete period of pulsation. The bottom axis shows the wavelength offset due to Doppler shift, from the nominal absorption line feature at around 4703.5Å. The top axis shows this converted into a velocity. The periodic shift of the absorption feature is qualitatively apparent and we could extract a velocity curve by simply picking off the line minima (red symbols) and plotting the corresponding velocities against time. However, the location of the line minimum is limited in accuracy and there are other spectral features whose information content is being ignored.

A better strategy is to use information from all such features simultaneously by measuring how much two spectra in the series overlap each other as one 'slides' over the other along the wavelength axis. If they are both similar, but simply wavelength-shifted versions of each other, there will be a large peak of 'overlap' at the shift increment. This is formalised by applying the mathematical operation of cross-correlation between the spectra. The conventional way of doing this is to use one spectrum as a 'template' against which the others are compared. However, it is possible to reduce the uncertainty in the outcome by using all pairwise comparisons within a spectrum set [4] which was the approach adopted here.

The results are shown in Figure 3. The plots have been referenced against the phase of the pulsation periods: for BE Lyn I used the ephemeris given in [5], for SZ Lyn that in [6]. All plots contain at least one complete period and partial data from a consecutive one (highlighted as red symbols). The velocities have been normalised to zero mean (so any systemic components have been subtracted).

The amplitudes and shape of the curves compare well with published data (see for example plots for BE Lyn in [7]). At the wavelengths measured, 0.1Å corresponds to a velocity difference of 6.4 km/s which is clearly visible here. In the original spectrum image, it corresponds to 2/3 of a pixel. The results for SZ Lyn are also comparable with those obtained by Leadbeater [8].

Summary: Commercially available amateur equipment is able to detect spectral Doppler shifts commensurate with radial velocities down to a few km/s in targets down to mag 8-9. It remains to see how far this magnitude limit can be pushed before reliable velocity estimates break down. Similarly, it will be of interest to see how the resolution of radial velocity measurement increases with brighter stars, and/or longer exposures (where permitted by the extent of the pulsation period).

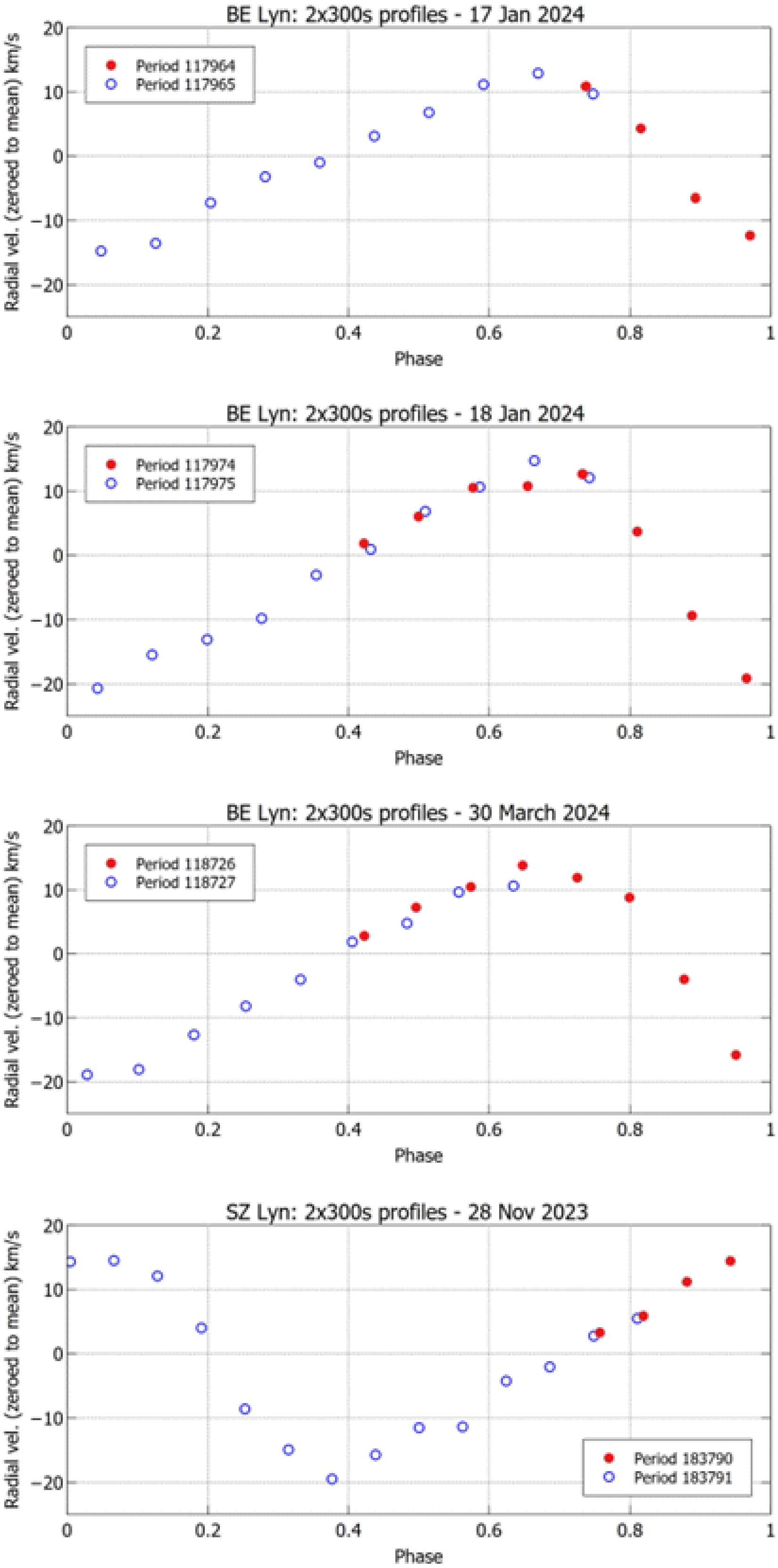

Figure 3: Radial pulsation velocities extracted by cross-correlation of spectra

1. *BAA Variable Star Section Meeting 2023 video 5 - Modelling Pulsating Stars by Phil Masding & Robin Leadbeater*, (Oct. 02, 2023). Accessed: Mar. 12, 2024. [Online Video]. Available: https://www.youtube.com/watch?v=Z865ow5BuTY
2. G. Handler, 'Delta Scuti Variables,' in *AIP Conference Proceedings*, American Institute of Physics, 2009, pp. 403–409. Accessed: Jun. 22, 2024. [Online]. Available: https://pubs.aip.org/aip/acp/article-abstract/1170/1/403/856833
3. C. Cavadore, 'Prism.' Alcor Systems. [Online]. Available: https://www.prism-astro.com/en/home/
4. C. A. Prieto, 'Velocities from Cross-Correlation: A Guide for Self-Improvement,' *Astron. J.*, vol. 134, no. 5, pp. 1843–1848, Nov. 2007, doi: 10.1086/522051.
5. J. Pena *et al.*, 'Binary nature of the HADS stars AN Lyn & BE Lyn,' *Rev. Mex. Astron. Astrofís.*, vol. 51, pp. 49–57, Dec. 2014.
6. P. J. H. *et al.*, 'OAN-TNT Results of Observations - Photoelectric Maxima of Pulsating Stars,' *Inf. Bull. Var. Stars*, no. 6220, Nov. 2017, doi: 10.22444/IBVS.6220.
7. A. Derekas *et al.*, 'Binarity and multiperiodicity in high-amplitude delta Scuti stars,' *Mon. Not. R. Astron. Soc.*, vol. 394, no. 2, pp. 995–1008, Apr. 2009, doi: 10.1111/j.1365-2966.2008.14381.x.
8. P. Masding and R. Leadbeater, 'Modelling Pulsating Stars,' in *Proceedings of the AAVSO 112th Annual Meeting*, Somerville, Mass., Dec. 2023.

CV & E News

Gary Poyner

garypoyner@gmail.com

Latest news on the new UGWZ star TCP J00003597+1757408, the outbursts of UV Per and UZ Boo, recoveries from minimum of the RCB stars AO Her, ES Aql and DY Per, and the summer fade of Z UMi.

Dwarf Novae:

A new dwarf nova in Pegasus (TCP J00003597+1757408), was discovered by Japanese observer Yuji Nakamura on July 05.706UT at magnitude 11.9C and announced on CBAT. Spectroscopic and photometric observations were reported by K. Isogai et al on Atel 16694 on July 6, with the conclusion that the new object is of type UGWZ. Kojiguchi-san posted a possible stage A superhump period of 0.0587(1)d from data by Brincat, Hambsch, Vihorlat Observatory team and Kyoto U. on vsnet-alert 28013 on July 16, 2024

BAAVSS observations are light (one observer, Poyner), but a visual inspection of the AAVSO light curve shows that the outburst lasted ~21d before fading to magnitude 17.5C.(Fig.1) A rebrightening occurred on July 29.9 to magnitude 15.1C, where it remains at time of writing (Augst 15).

The object can be found at J2000.0 00 00 35.97 +17 57 42.8, and charts are available from the AAVSO chart plotter. Be aware that the AAVSO chart has the variable plotted further to the East than it actually appears. I did report this to the AAVSO as soon as I realised without acknowledgment.

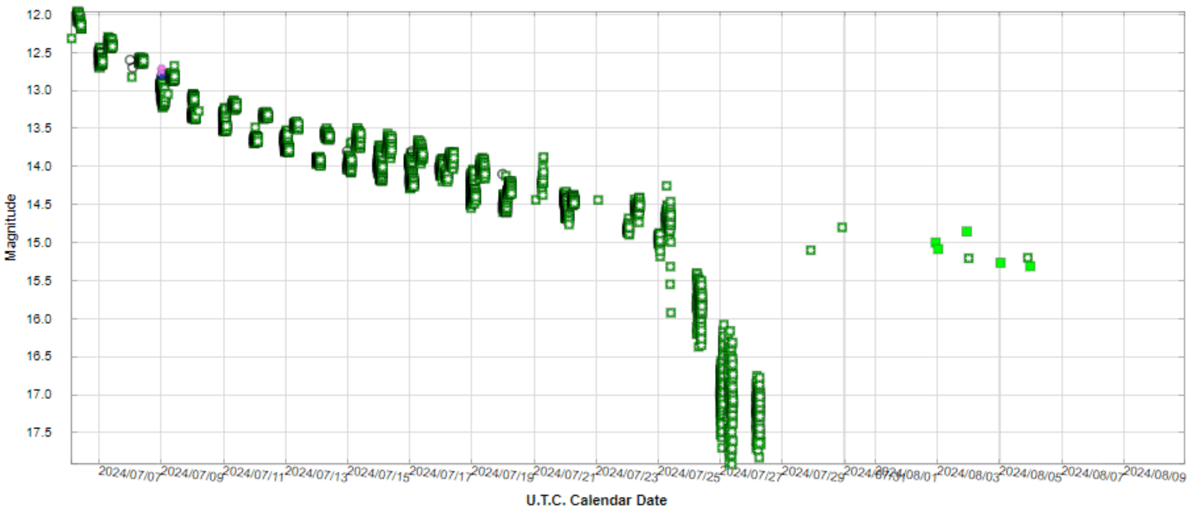

Figure 1: AAVSO light curve for TCP J00003597+1757408. July 06 - Aug 05

UV Per

The first outburst of this popular UGSU star seen since June 2020, was detected by Belgian observer Eddy Muyllaert on July 27.979UT at magnitude 12.3 visual and announced on CVnet on July 28.0UT. Three BAAVSS observers contributed to the light curve, with special mention to Ian Sharp and Magnus Larsson for their extended time series coverage back to minimum magnitude. The outburst was over pretty quickly, fading from 12.6 visual on July 27 to 16.5V mean by July 29 and eventually 17.85V mean by August 7. No rebrightenings were observed, and we can conclude from this that the outburst was a normal one, rather than a superoutburst.

A number of comments, plots and outburst images relating to this outburst can be seen on the BAA forum.

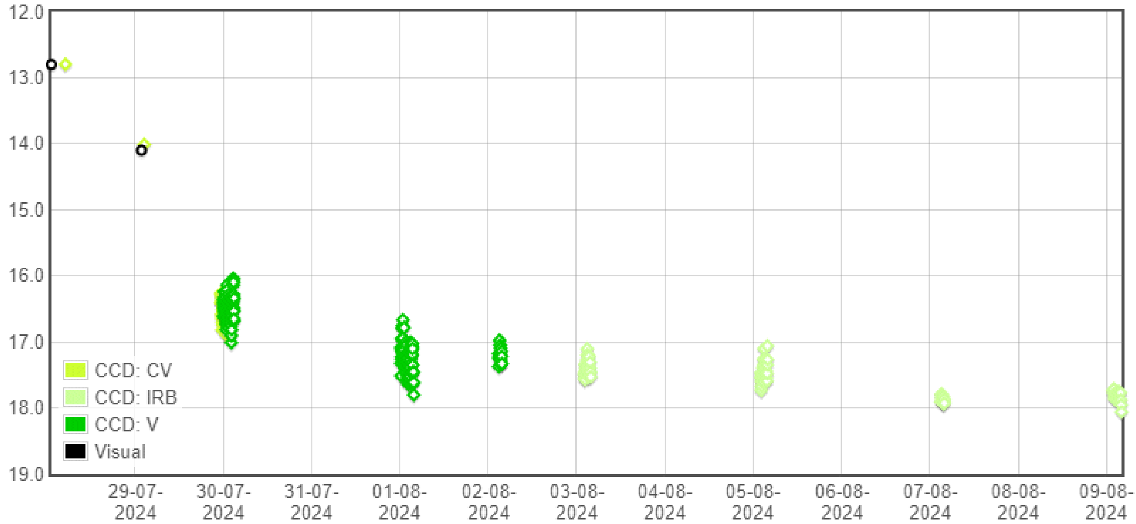

Light curve for UV Per – July 26 - Aug 15. *BAAVSS database.* Observers M. Larsson, G. Poyner I Sharp

UZ Boo:
The first major outburst since March 2019 (there was a brief minor outburst to 16.1TG recorded in April 2023) was detected by Japanese observer Masayuki Moriyama on Aug 08.531 UT at magnitude 12.91C and reported on vsnet-outburst 31039. The outburst seems to have peaked several hours later on Aug 08.886 UT at visual magnitude 11.8 (AAVSO), and at the time of writing (August 16), UZ Boo had faded to magnitude 12.88C. Unusually there have not been any observations yet reported of the detection of superhumps on vsnet, possibly because of UZ Boo's location in the western evening sky at this time. Good CCD coverage from BAA observers Denis Buczynski, Magnus Larsson and Ian Sharp with Larsson detecting 0.1 mag superhumps on Aug 17. Hopefully we may have more to report in the next VSSC as this outburst is still in its early stages. Discussion and plots may be followed on the BAA forum.

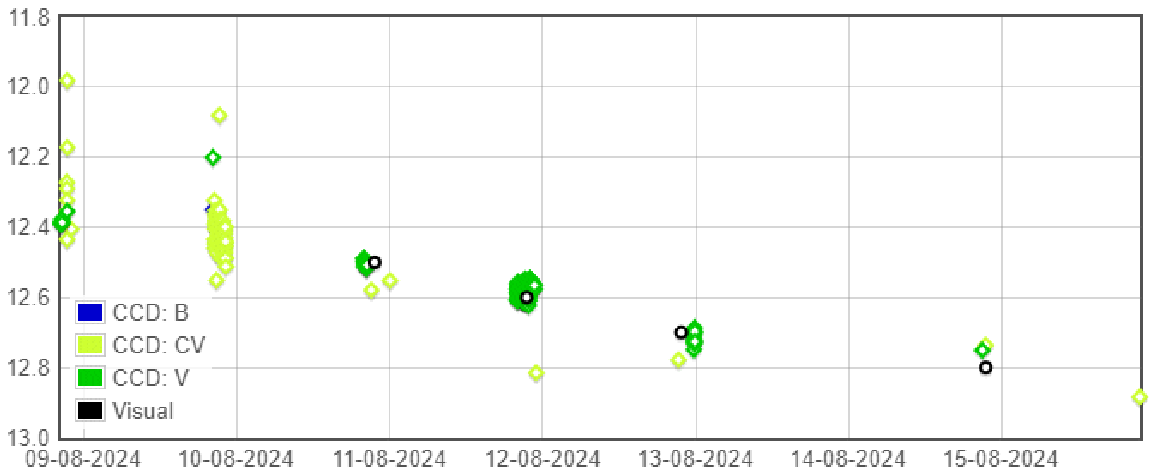

Light curve for UZ Boo, Aug 07-16. *BAAVSS database* Observers; D. Buczynski, M Larsson, PC Leyland, G Poyner, I Sharp.

RCB News:

It's been a busy time of late for followers of RCB stars, with a number of BAAVSS targets hitting the activity button over the past few months.

Both ES Aql and AO Her are recovering from deep fades over the past 12 months and are well on their way to maximum magnitude again. AO Her had a fairly long minimum lasting from May to December 2023 around magnitude 18.0-18.5C before a recovery was detected in January 2024, which reached magnitude 13.2C in March before fading again to 16.0C in May 2024. From then AO Her has recovered to magnitude 12.2C in early August and is once again visible in smaller telescopes.

ES Aql has made a fairly rapid recovery from the fade reported in VSSC 200, rising from magnitude 17.6C on May 21 2024 to 12.17C by August 11. Maximum brightness for ES Aql is between magnitudes 11.0 and 12.0 and is once again visible in small telescopes.

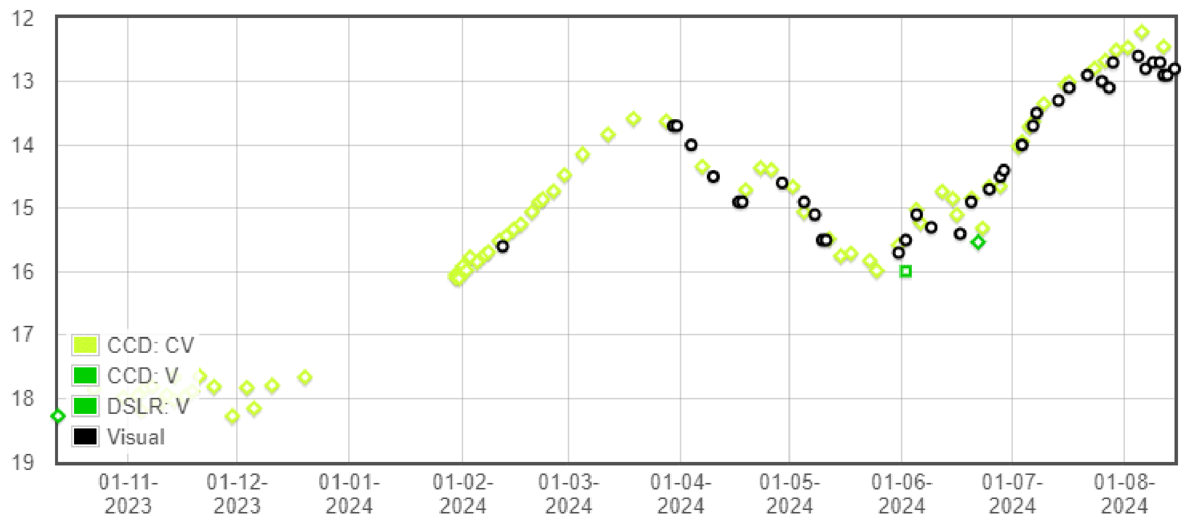

AO Her. Oct 01, 2023 to Aug 16, 2024. *BAAVSS database.* Observers W Parkes, G Poyner, GJ Privett, IL Walton

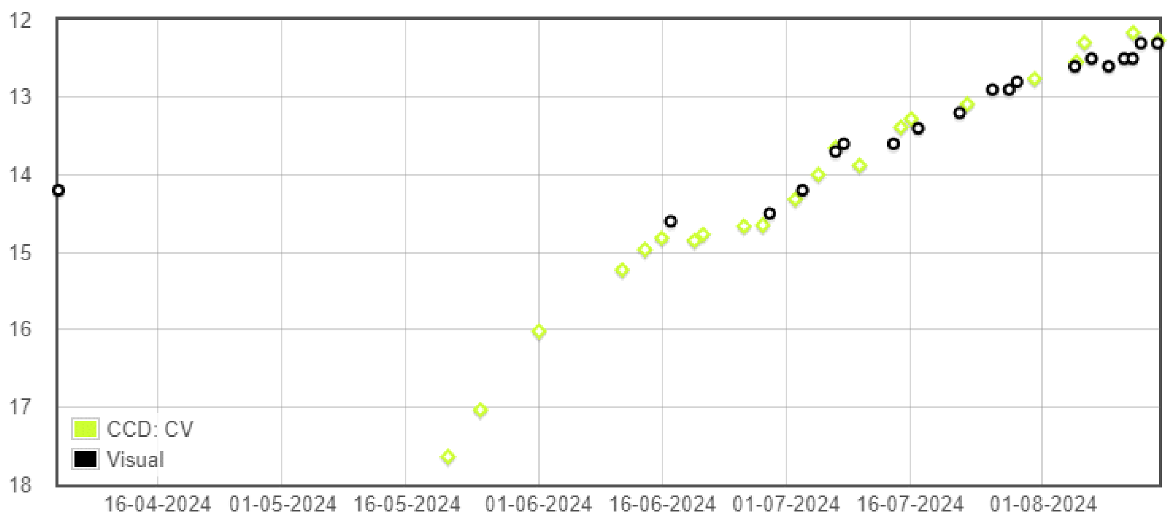

ES Aql. Apr 01 2024 to Aug 16 2024. *BAAVSS database*. Observer G Poyner

As reported in VSSC 200, DY Per began its first fade for two years in December 2023, reaching magnitude 15.0 visual by mid-April, when the field was lost in the northern sky. DY Per was picked up again in late June at magnitude 15.5V, with a recovery to magnitude 14.3V by mid-August. A visual inspection of the light curve suggests a minimum of 16.0 in early May. This recovery should be well covered from this time as DY Per becomes more favourably placed in the late Summer sky.

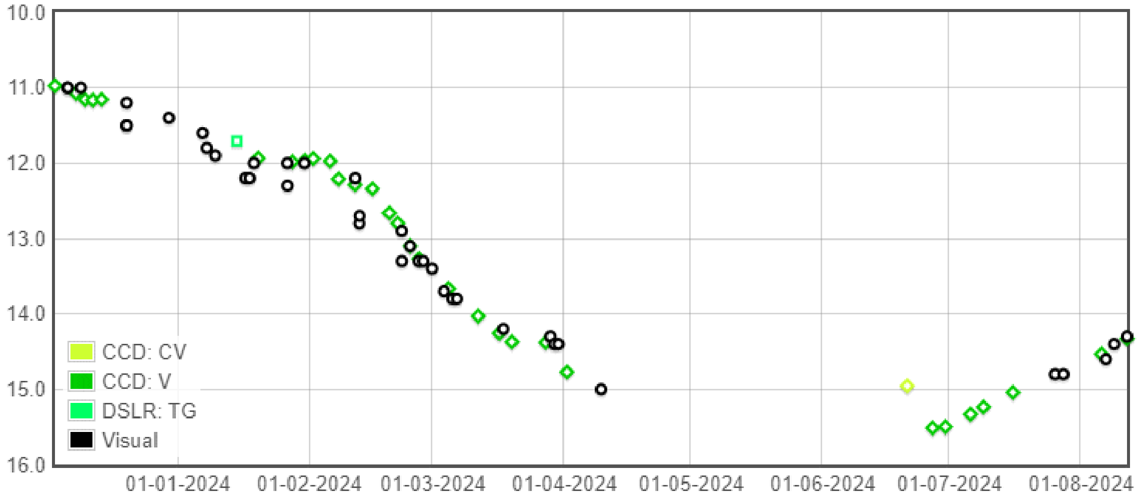

DY Per December 1, 2023 to Aug 16, 2024. BAAVSS database. Observers: JT Bryan, RC Dryden, W Parkes, G Poyner, T Vale, PB Withers.

The historically long maximum of Z UMi was mentioned in VSSC 195, along with some speculation as to when this long bright state might end with a fade. Finally, after 1,400+ days Z UMi has begun to decline. There were signs that something may be happening in late July with a drop to magnitude 11.5mv, and since that time a slow regular fade to 13.1mv by August 14 has set in. This decline rate is consistent with previous fades with this star. In the past, when Z UMi had faded to magnitude 13, the fade continues to magnitude 15 or just below, so there may be some way for Z UMi to go yet. The deepest fade ever recorded occurred in August 2007, when magnitude 19.0C was reached – although this is the historically deepest level yet reached.

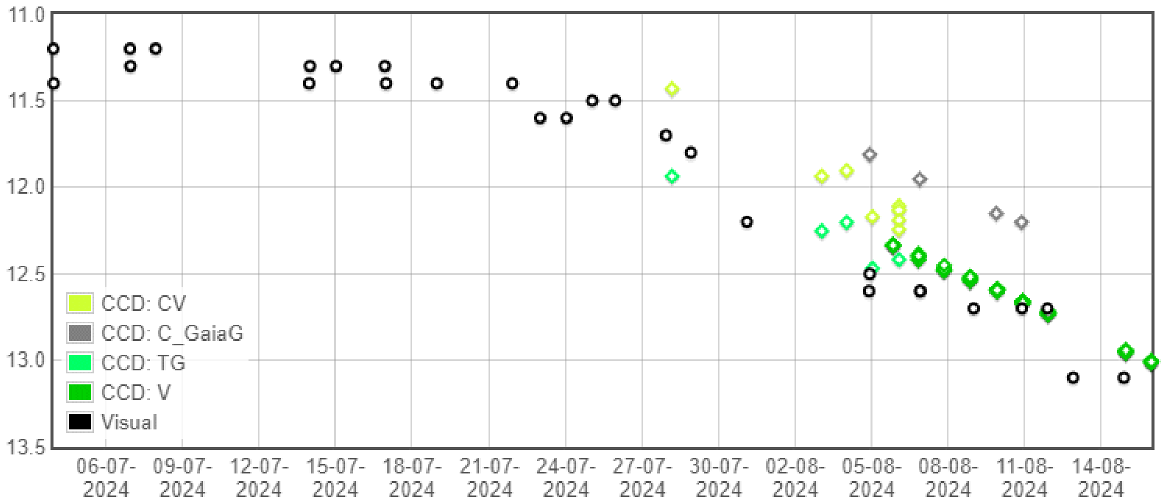

Z UMi July 1 to August 16, 2024 *BAAVSS database*. Observers: ND James, G Poyner, I Sharp, J Toone, IL Walton, PB Withers.

Observations of the recent transient AT 2024lwu = TCP J20023703+3947002

Christopher Lloyd, Magnus Larsson, Ian Sharp, Maxim Usatov, Gary Poyner and Stewart Bean

The recent outburst of the transient AT 2024lwu is shown to be SU Ursae Majoris-type superoutburst. Previous outbursts are identified in the ATLAS data as normal and UGSU superoutbursts. Time-series data show a periodic variation with an amplitude $0^m.1$, near $0^d.0771$ or $0^d.0715$ during the second half of the plateau phase that are consistent with superhumps. The transient at quiescence is identified with a star at 0.7 arcsec from the published discovery position.

The recent outburst of the transient AT 2024lwu = TCP J20023703+3947002 was discovered on 2024 June 20.27 (JD = 2460481.77) by Kumar (2024) (Golden Ears Observatory Transient Survey – GEOTS) at *CV* = 16.6, on three 30-second unfiltered exposures using a 0.36-m f/2 Schmidt-Cassegrain + CCD. Although no confirmation spectra were taken at the time, its position in Cygnus at galactic latitude *b* = +4.75 and its brightness, immediately suggested that it was a CV rather than an extragalactic transient. The field is very crowded and in particular there is a faint star at 3 arcsec from the position of the transient for which *Gaia* gives *G* = 18.83 and ($G_{BP} - G_{RP}$) = 1.56. For the same star Pan-STARRS gives *g* = 19.62 and (*g* − *r*) = 0.87. The transient is now listed as a UG variable in the AAVSO VSX under the TCP designation.

Follow-up observations began immediately and showed that after an initial fade the transient had returned to its outburst brightness and was remaining bright. A search through archival data also showed that there had been previous outbursts, suggesting that the transient was an SU Ursae Majoris system (UGSU) (Lloyd & Usatov, 2024). Further photometry was taken over the following days as the outburst was monitored through the relatively constant plateau phase and the eventual fade to quiescence.

The Asteroid Terrestrial-impact Last Alert System (ATLAS) project has observed AT 2024lwu since 2015 in the 'cyan' *c* band (420–650nm), and the 'orange' *o* band (560–820nm), and the data were downloaded from the ATLAS Forced Photometry web service (Tonry et al., 2018, Shingles et al., 2021). The observations in 2015 and 2016 are extremely sparse, but the bulk of the coverage is relatively even from 2017 with a median cadence of 2.0d in the orange band and 4.0d in the cyan (c) band. Data from the Zwicky Transient Facility (ZTF) (Bellm et al., 2019, Masci et al., 2019) are also available in the Sloan *g* (414–546nm) and *r* (566–721nm) passbands, but these are almost exclusively from 2018 and 2019, and do not cover any of the previous outbursts. Also, the ZTF data are over a magnitude brighter than the closest ATLAS bands, and are probably entirely due to the faint companion, so these have not been used.

The complete light curve from the ATLAS survey and recent photometry is shown in Fig. 1. The median ATLAS magnitudes are *o* = 20.0 and *c* = 20.5, with a range of about one magnitude in both bands. These are over a magnitude fainter than the close companion suggesting that blending is not a significant issue. In addition to the current outburst there are another three coherent groups of observations brighter than magnitude 18.0, plus one other single night with multiple observations. All of these runs point to additional outbursts, and the two best observed are shown in Fig. 2. The run from 2016 contains all five of the observations from that year and shows a linear decline of one magnitude from *c* = 16.9, over 9 days. The second example is the outburst from late 2023 that rose

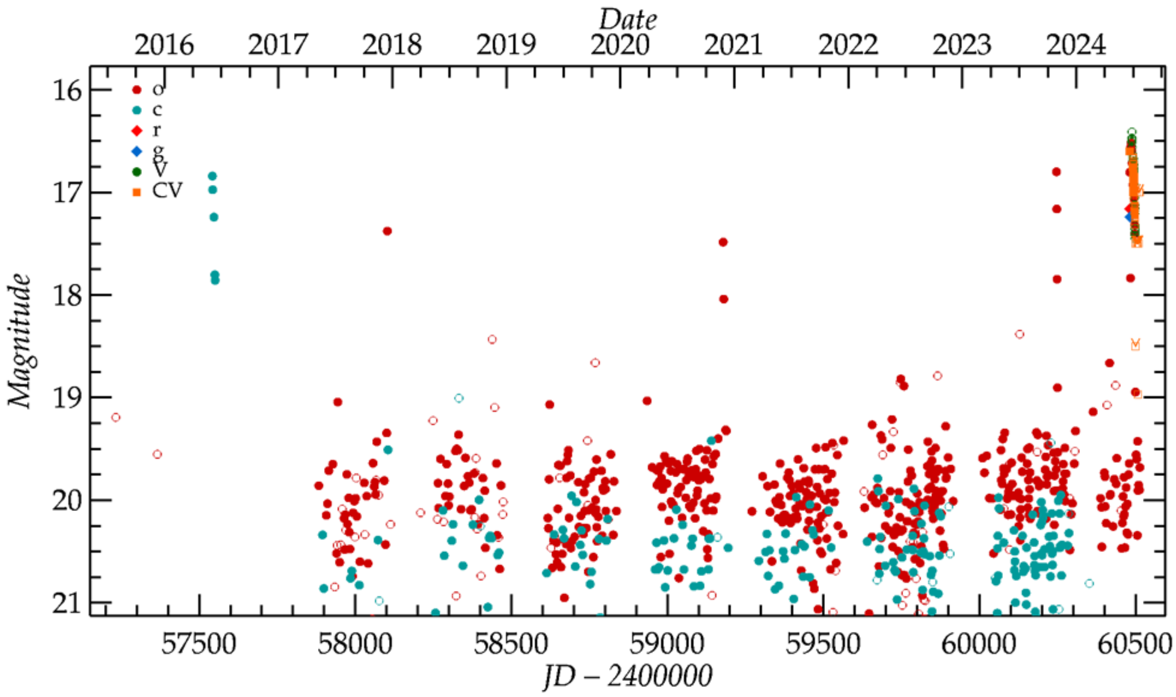

Figure 1: The complete light curve of AT 2024lwu showing, mostly, the archival data from ATLAS in the orange (o) and cyan (c) bands. The other bands only appear for the most recent outburst. The filled symbols are means of multiple observations, and therefore carry more weight.

from quiescence at $o \simeq 19.8$ to $o = 16.8$ in one day, and then faded rapidly back to quiescence in another 4–5 days. These two alone strongly suggest SU Ursae Majoris-type normal and superoutbursts. The other two previous outbursts are not well covered, but one is short ~ 4 days, while the other is poorly constrained.

Apart from Kumar's initial observation, only two other measurements have been reported and these come from one day after discovery (Balam & Hess, 2024). Together with contemporaneous ATLAS data these showed that the transient had faded dramatically by $1^{m}.2$ over the 2 days into the outburst. The observations reported here began some four days later, after the ATLAS data showed that the transient has returned to its discovery brightness. Over the following days, time-series runs, shorter

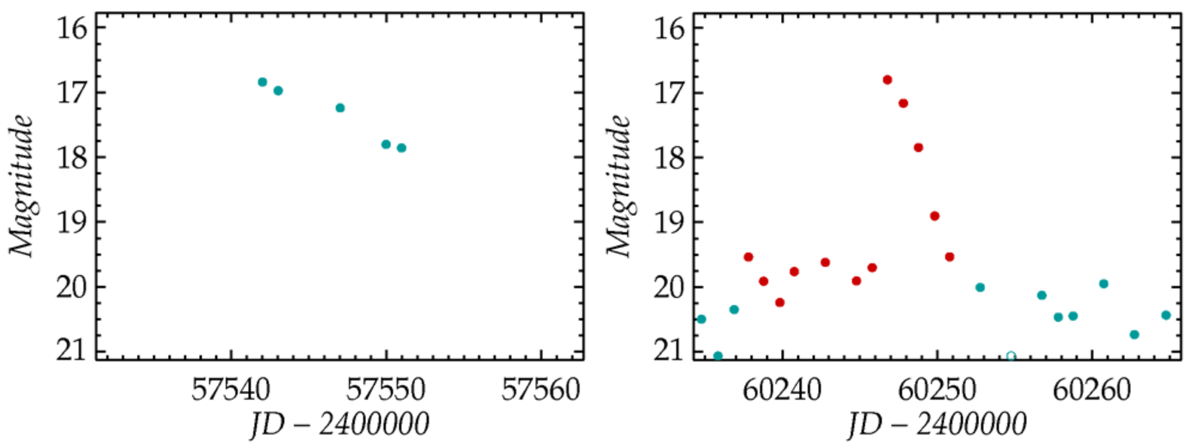

Figure 2: Epoch plots of two previous outbursts from 2016 (left) and 2023 (right). The 2016 outburst shows a linear decline of one magnitude over 9 days and is typical of the plateau phase of a SU UMa superoutburst. The 2023 outburst is equally bright, but the whole event is completed in 5 days, and is typical of a normal SU UMa outburst. The symbols are as in Fig. 1.

Table 1: Details of the observers and equipment used

Observer	Observatory/site, telescope, detector, bands
Bean	SLOOH CANARY 2 CDK17 + FLI PL16803 unfiltered
Larsson	CDK17 + ASI6200 unfiltered
Poyner	SLOOH CANARY 2 CDK17 + FLI PL16803 unfiltered
Poyner	COAST III CDK17 + FLI ProLine KAF-09000 unfiltered
Sharp	PixelSkies C11 + SX694 Trius Pro with 'Luminance' IR Blocking (CV) and V
Usatov	Alnitak CDK17 + Moravian Instruments C3-61000 with V filter

groups and individual observations were made with a variety of remotely controlled telescopes in locations in mainland Spain and the Canary Islands. The facilities used by the different observers are listed in Table 1, and the observation log of the time-series runs and multiple observations are given in Table 2. In addition to these a number of individual observations were made. All the observations are available from the AAVSO or BAA VSS databases.

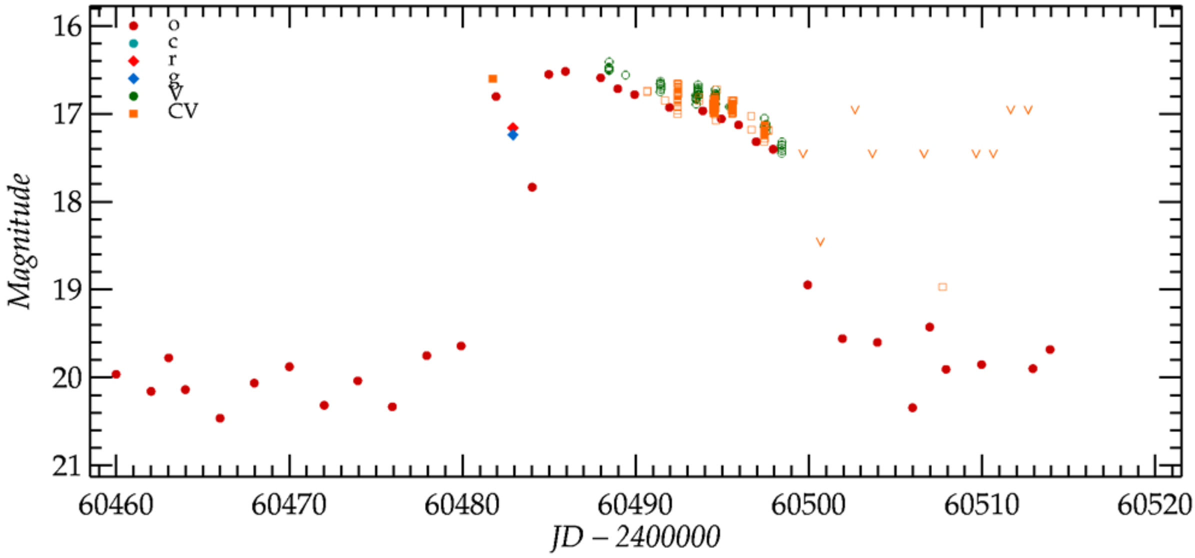

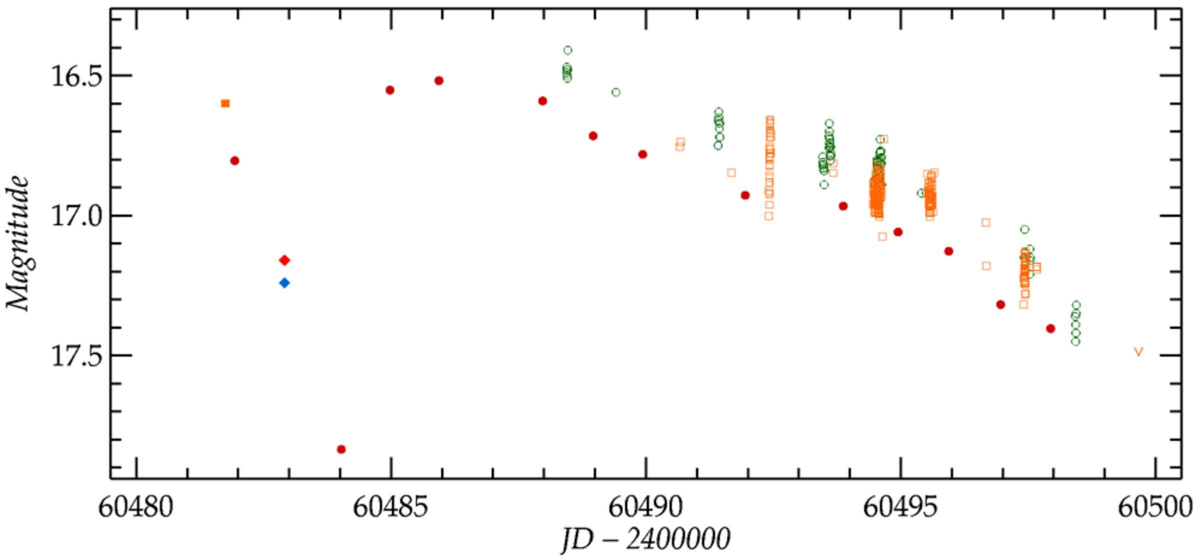

Figure 3: Light curve of the recent outburst showing it in a wider context (top), and the expanded detail of the precursor outburst and the plateau phase prior to the final fade (bottom).

The light curve covering the recent outburst is shown in Fig. 3 where it can be seen that the system brightened from quiescence at $o \sim 20.0$ and was detected in outburst less than two days later. As mentioned earlier the brightness then drops by more than a magnitude over the next two days before rebounding to the peak brightness of $V \simeq 16.5$ another day later. Such behaviour is typical of a precursor outburst in SU UMa systems. The system then remained close to peak brightness for about four days and then faded by about one magnitude during the rest of the plateau phase, before finally dropping to the quiescent level. In total the plateau phase lasted for $\simeq 14$ days and was preceded by another 3–4 days of the precursor outburst, so even by superoutburst standards this was a substantial event. However, the amplitude of the outburst is only 3.5 magnitudes, which is relatively low for a UGSU superoutburst. Of the 968 UGSU systems listed in the AAVSO VSX the median amplitude is 5.8 magnitudes, and only 4.9% have amplitudes < $3^{m}.5$, so the quiescent magnitude may be inflated. The magnitudes from the ATLAS Forced Photometry Server are determined on the position given, using the PSF of the image, and this typically has a FWHM $\simeq 5$ arcsec. So, in this case the star at 3 arcsec will be partially included in the profile and the quiescent magnitudes will be inflated.

Closer examination of the time-series observations shows significant short-term variation that appears to be superhumps. The best observed runs are shown in Fig. 4, but unfortunately there is only one night with sufficiently long runs, however, this does demonstrate the nature of the variation. The issues with identifying the superhump period are, (1) that the amplitude clearly decreases through the outburst, and (2) the level changes from night to night, and between bands, so aligning the light-curve fragments is problematic. Also, the period will evolve through the outburst. Trial periods were

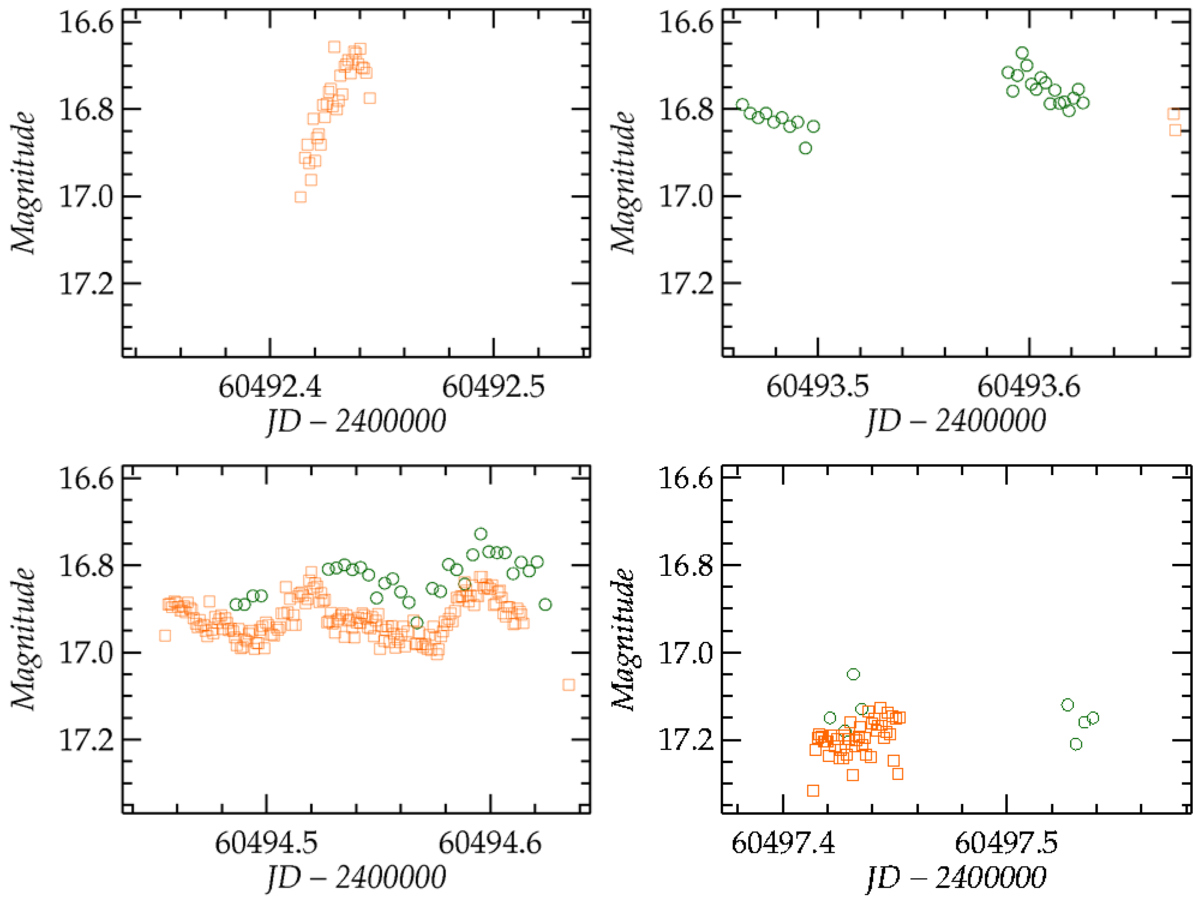

Figure 4: Details of the individual time-series runs plus other contemporaneous observations.

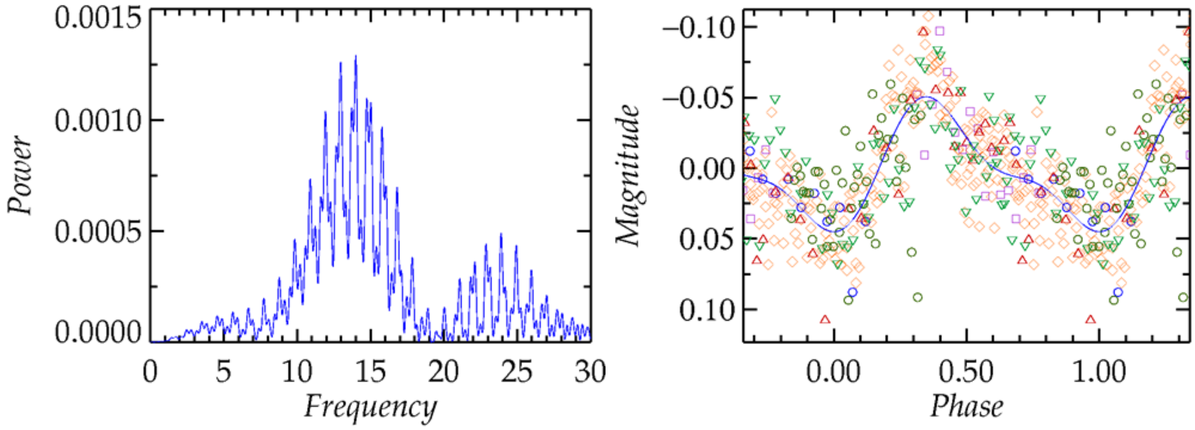

Figure 5: The Discrete Fourier Transform periodogram of the longer time-series runs (left), and the same selection of data folded on the f =12.97cd^{-1} or 0^{d}.0771 period. The symbols identify different runs.

identified through the Discrete Fourier Transform (DFT) periodogram of several subsets of the data centred on the long run on 2024 July 2 (JD = 2460494). These were then fitted with a 2-harmonic Fourier series – as the variation is clearly not a simple sinusoid – to determine the fit with the lowest rms residual. The run on JD = 2460492 was not included initially as its large amplitude is inconsistent with the other variations. The best solutions quickly resolved to a series of 1-day aliases of a frequency near 12.9cd^{-1}. Different subsets yielded slightly different fits, but the two best frequencies in all cases were near 12.97 and 13.99cd^{-1} or 0^{d}.0771 and 0^{d}.0715. The DFT periodogram of the longer time-series runs is shown in Fig. 5 together with the same data folded on the f = 12.97cd^{-1} or 0^{d}.0771 period, by way of illustration.

Table 2: Details of the time series runs and other multiple observations

Date UT	HJD	Hours	Band	n	Observer
2024 Jun 26	2460488.445 - .468	0.5	V	7	Usatov
2024 Jun 29	2460491.414 - .451	0.9	V	11	Usatov
2024 Jun 30	2460492.414 - .445	0.7	CV	34	Larsson
2024 Jul 01	2460493.465 - .499	0.8	V	10	Usatov
2024 Jul 02	2460493.591 - .626	0.9	V	17	Sharp
2024 Jul 02	2460494.455 - .616	3.8	V	181	Larsson
2024 Jul 02	2460494.487 - .498	0.3	V	4	Usatov
2024 Jul 03	2460494.528 - .625	2.3	V	27	Sharp
2024 Jul 03	2460495.404 - .497	2.2	V	2	Usatov
2024 Jul 04	2460495.527 - .626	2.4	CV	58	Sharp
2024 Jul 05	2460497.414 - .453	0.9	CV	45	Larsson
2024 Jul 05	2460497.422 - .539	2.8	V	8	Usatov
2024 Jul 06	2460498.424 - .443	0.5	V	6	Usatov
2024 Jul 06	2460497.660 - .666	0.1	CV	2	Poyner

The other remaining question is whether the star can be identified at quiescence. In addition to the companion at 3 arcsec, two surveys The Pan-STARRS1 (PS1) release (2016) and UKIRT Infrared Deep Sky Survey (UKIDSS) Galactic Plane Survey (GPS) Release 6 (2012) provide independent, but very partial information on another, even fainter star at 0.7 arcsec – from the discovery position of the transient. From all the Alnitak images the mean position of the transient has been measured as α = 300.654420(37) δ = +39.783120(17) J2000, with internal errors of ±0.10 and ±0.06 arcsec in RA

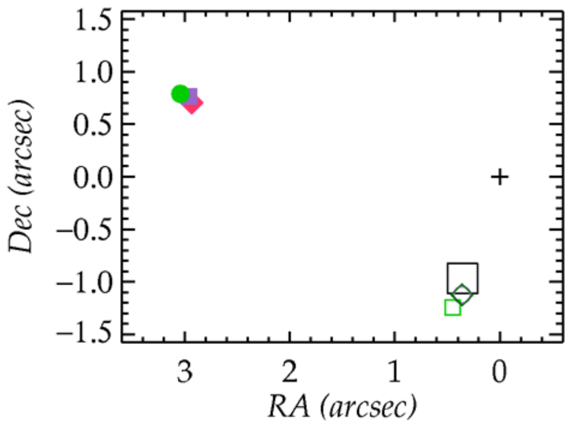

Figure 6: The position of the transient measured on the Alnitak images (large square) relative to the published position (+). Similarly, the relative positions of the 3-arcsec star (filled symbols) and the 0.7-arcsec star (other open symbols) from the catalogues mentioned.

and Dec respectively. The formal errors on the astrometric solutions are all rather larger at close to ±0.45 arcsec. The location of this position and those of the 3- and 0.7-arcsec companions from the catalogues mentioned, plus *Gaia* are plotted on Fig. 6, relative to the published position of the transient. It is clear that the transient at quiescence is actually the star at 0.7 arcsec. Magnitudes are only available in Sloan *z* and *y*, and 2MASS *J*, and suggest that the star is very red. In *g* or *r* the magnitude is probably no brighter than ∼22, so this star would provide a more typical outburst amplitude for a UGSU system.

In summary, AT 2024lwu is shown to be a new UGSU system. It shows the typical UGSU normal and superoutbursts, and in the case of the most recent outburst, also shows a clear precursor as well. Periodic variations during the plateau phase are interpreted as superhumps, with a period most likely near $0^d.0771$ or $0^d.0715$, but the other nearby 1-day aliases at ≃ 12 or 15cd^{-1} are not excluded. The quiescent magnitude of the system in the ATLAS data is inflated by the close companion at 3 arcsec, which is partially included in the photometric profile. The transient at quiescence is identified with the star at 0.7 arcsec from the initial discovery position, giving an outburst amplitude of at least 5 magnitudes.

The authors are pleased to acknowledge use of NASA's Astrophysics Data System Bibliographic Services. This research has made use of the SIMBAD database and the VizieR catalogue access tool operated at CDS, Strasbourg, France. The authors gratefully acknowledge use of the AAVSO Variable Star Index (VSX). This work has made use of data from the Asteroid Terrestrial-impact Last Alert System (ATLAS) project. The ATLAS project is primarily funded to search for near earth asteroids through NASA, Kepler/K2 and STFC grants.

References

Balam, D. D. & Hess, E., 2024, *Transient Name Server AstroNote*, **163**, 1
Bellm, E. C., Kulkarni, S. R., Barlow, T., et al., 2019, *PASP*, **131**, 068003
Kumar, B., 2024, *Transient Name Server Discovery Report*, **2024-2028**, 1
Lloyd, C. & Usatov, M., 2024, *The Astronomer's Telegram*, **16676**, 1
Masci, F. J., Laher, R. R., Rusholme, B., et al., 2019, *PASP*, **131**, 018003
Shingles, L., Smith, K. W., Young, D. R., et al., 2021, *Transient Name Server AstroNote*, **7**, 1
Tonry, J. L., Denneau, L., Heinze, A. N., et al., 2018, *PASP*, **130**, 064505

rho and tau Cassiopeiae

Colin Henshaw

cohensn1987a@hotmail.com

An analysis of observations of rho and tau Cassiopeiæ made in an attempt to determine if tau Cassiopeiæ is variable. Rho Cassiopeiæ was used as a control as it is an established variable star that can be expected to vary.

Tau Casiopeiæ was used as a comparison star for rho Cassiopeiæ for many years, but as far back as 1969 I found its magnitude didn't agree with that in the sequence. I suspected it of variability, (Henshaw 1973) and my suspicions were further aroused when my friend in the United States, Peter Quadt, independently suspected it. Later Peter Hornby also said he suspected it. I analysed observations of tau Cassiopeiæ made by myself and Hungarian observers but could not find anything conclusive (Henshaw 1974, 1976). In Percy (1985) he undertook to observe the star photometrically between June 25th 1979 and November 17th 1980 and concluded it was not variable. What can really be concluded was that it had not varied between those two dates. The fact that three observers suspected independently made it suspicious, and I was not totally convinced. By the time I went to Saudi Arabia I had acquired a couple of Canon digital cameras and was now able to monitor the two stars on a regular basis. A 135mm Carl Zeiss lens was used set at f5.6, and each image was exposed for five seconds at 400ASA. For each data set eleven images were taken, along with ten dark frames, and these were measured after dark frame subtraction, using the photometry tool on AIP4Win and double checked. The images then plotted on an Excel spreadsheet which averaged out the results and plotted them out on a light-curve. The period covered was from 2013 to 2022. Two comparison stars were selected, sigma Cassiopeiæ at 4m.88, and SAO 35761 (HR 9010) at 5m.55, the latter being the same comparison used by Percy. Rho Cassiopeiæ was used as a control as it is an established variable star and could be expected to vary. The light curve shows rho Cassiopeiæ above and tau Cassiopeiæ below. Rho Cassiopeiæ was obviously variable, showing pseudo-periodic waves between 4m.3 and 4m.9, while tau Cassiopeiæ was effectively constant.

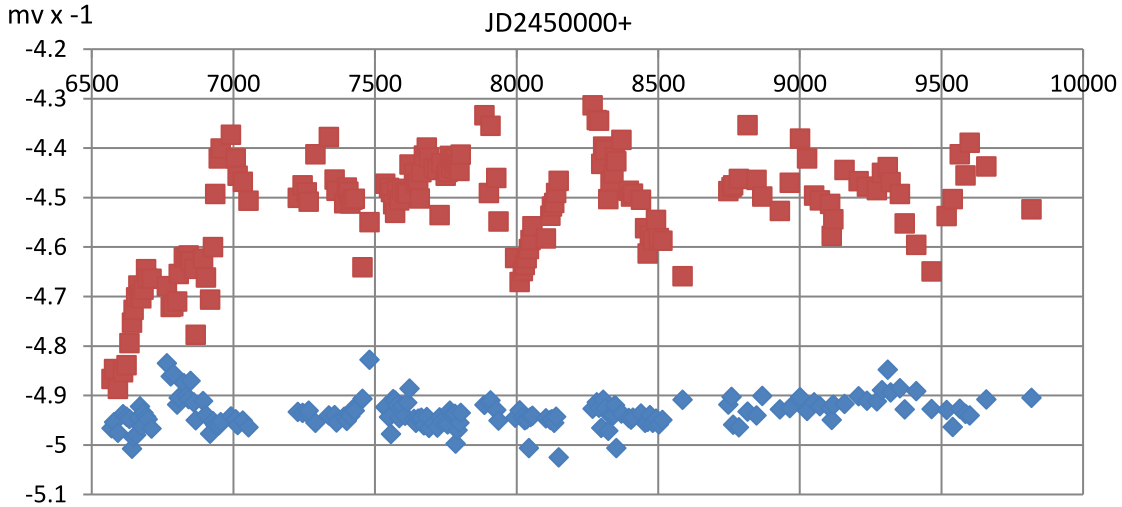

Unfortunately, it is not possible to prove a negative. Just because tau Cassiopeiæ did not vary between 2013 and 2022 does not mean conclusively that it is constant. It just states that it was constant during the period of observation. Three observers did have doubts about it in the late 1960s and early 1970s so it will always be under suspicion, though I tend to agree with Percy's conclusion that it is constant. If so, then it may be safe to reinstate it as a comparison for rho.

References:

Henshaw, C., 1973 The Astronomer, 10, 15.

Henshaw, C., 1974 Albireo 44, 20 – 21.

Henshaw, C., 1976 Light-Curve 1, 5.

Percy, J. R. Tau Cassiopeiæ – Not a Variable Star JAAVSO 14, 2 42 – 54.

Should individual amateurs join the big-data era?

Paul Leyland

paul.leyland@gmail.com

A SQL database schema and a suite of Perl scripts have been written to facilitate analysis of images of the fields of variable stars. To the extent possible, all stars within each image are measured photometrically and the results stored in the database, along with positional and identification data. To date most amateur astronomers neither collect nor analyse all this data, thereby discarding much of the information which may be present. Examples are given which suggest that productivity may be increased several-fold over the traditional approach.

Many (most?) professional astronomers have to fight against intense competition to acquire a relatively small amount of telescope time. In consequence, they generally try rather hard to extract as much information as they can from the limited data they manage to collect. Many (most?) amateur astronomers are able to spend as much time as they wish to observe their objects of interest and their incentive to extract everything possible is generally quite small, possibly non-existent. I believe that amateurs can learn a great deal from professionals in this respect.

In the particular case of photometric observation of variable stars, a single image will typically record somewhere between a few dozen and a few thousand stars. It appears to be rare for more than a single target variable and a few sequence members to be measured. What a dreadful waste of time, effort, data and potential for extracting scientifically useful information! Leaving aside the possibility of characterizing asteroids which may happen to be passing by, a typical image may contain several other known variables within its boundaries (and dozens in the case of variables in near-by galaxies). Who knows how many undiscovered variable stars might be uncovered if only the data were to be fully analysed?

I have been as guilty as most amateurs in this respect. To atone for my sins, I have recently written software to record a great deal of data which can be extracted from my image archive and from images which are subsequently acquired from night to night. The major components are a PostgreSQL database to hold the data and a few scripts to extract it from images.

The database has four principal tables: a star catalogue based on a limited sub-set of the Gaia-DR2 catalogue; a table of sequence information in three bands (Johnson B, Johnson V and Cousins R) downloaded from AAVSO; a list of known variable stars; and a record of every photometric measurement of every measurable star in every image processed. A column in this last table records whether or not the corresponding measurement has been uploaded to the BAAVSS photometry database. All tables have a last-updated column for use should later debugging be needed.

When each new variable is to be processed a script downloads the positions, IDs and G magnitude data of every star in the Gaia-DR2 catalogue within 20 arc minutes. The script also downloads the sequence data (ID, position and tri-band magnitudes) for that variable and correlates it with the Gaia-DR2 positions. Further, it downloads the names and positions of every known variable within 15 arc minutes of the prototype VS. These sizes are arbitrary limits based on the field of view of my imaging system.

A second script queries the database for the positions of every star which lies within the limits of an image to be analysed; it produces a source list file in the format expected by Russ Laher's *Aperture Photometry Tool* (APT). The file may contain somewhere between a few dozen and a few thousand lines, depending primarily on the galactic latitude of the area imaged.

APT is then run interactively on the image and a comma-separated-variable format file produced which contains the photometric data on all the stars specified by the source list. Eventually, it is hoped, this stage may also be scriptable. At present vagaries of image quality, tightness of focus, image scale, and the like, have proved to be too challenging for reliable automation.

The final script performs ensemble photometry using the stored sequence data and then uploads to the database both the instrumental and computed magnitude with their errors so long as the latter error does not exceed an arbitrarily chosen 0.15 magnitudes. The Julian Date at the time of observation and the filter used are, of course, part of the information uploaded.

A subsidiary script can stack sub-images to produce a co-added image for photometric analysis. It carefully sets an exposure-weighted value for the mid-exposure time of the composite image.

I have something over 22,000 images which have been collected between 2018 and 2020. All are stored on disk and much of the meta-data extracted from their FITS headers is held in another PostgreSQL database. The great majority of the images were taken to study a single variable star in each frame. Only a small proportion have yet been processed by the pipeline described above. During development of the software, five carefully chosen variables were processed. These are AL Com, LS And, DY Per, Mrk 421 and V742 Lyr. Two (LS And and AL Com) were too faint to be measured on least some of the images; the others were bright at the time of imaging; a field star of Mrk 421 is saturated in its image; AL Com has a bright galaxy (M88) in the field; DY Per lies in a dense part of the Milky Way whereas AL Com is in a rather barren part of the sky. This set is small enough to be described in detail below.

After those five had been processed the database contained 31961 stars (19750 in the vicinity of DY Per alone) and 20 variables. It will be noted that 80% of the latter are field variables. From 16 stacked images 11297 measurements were made of 3899 distinct stars —almost all of which have not yet been examined in any detail. It seems likely that these records will be a rich seam for data mining of previously undiscovered variable stars. A future article will address this issue.

The results of a few SQL queries should give a flavour of the information available for in-depth examination. The first gives the names of variables located in the five fields and their identifiers in the star catalogue table.

```
SELECT * from variable.
 var_id |            name            | star  |          updated
--------+------------------------------+-------+----------------------------
      1 | CSS_J003233.0+420013         |  3273 | 2020-05-13 21:42:03.535185
      2 | CSS_J003059.7+420151         |  2644 | 2020-05-13 21:42:03.535185
      3 | CSS_J003229.3+420354         |  3838 | 2020-05-13 21:42:03.535185
      4 | CSS_J003149.5+415203         |  1231 | 2020-05-13 21:42:03.535185
      5 | LS And                       |  1764 | 2020-05-13 21:42:03.535185
      6 | CSS_J003115.3+420059         |  2012 | 2020-05-13 21:42:03.535185
     15 | ASASSN-V J023406.90+560616.3 | 29789 | 2020-05-15 18:29:00.11541
     16 | DY Per                       | 38265 | 2020-05-15 18:29:00.11541
     17 | ASASSN-V J023642.16+560334.3 | 34302 | 2020-05-15 18:29:00.11541
     18 | DX Per                       | 40238 | 2020-05-15 18:29:00.11541
     19 | GPX-TF8A-630                 | 34682 | 2020-05-15 18:29:00.11541
     20 | GPX-TF8A-1104                | 39785 | 2020-05-15 18:29:00.11541
     21 | DZ Per                       | 35811 | 2020-05-15 18:29:00.11541
     22 | CzeV662                      | 34299 | 2020-05-15 18:29:00.11541
     24 | AL Com                       | 44468 | 2020-05-17 12:01:58.950564
     26 | NSV 18598                    | 45208 | 2020-05-17 13:56:09.605762
     27 | CSS_J110333.9+380837         | 45249 | 2020-05-17 13:56:09.605762
     28 | MRK 421                      | 45313 | 2020-05-17 13:56:09.605762
     31 | V0742 Lyr                    | 58074 | 2020-05-17 16:59:24.411295
     32 | PS1-3PI J183822.19+471705.4  | 53927 | 2020-05-17 16:59:24.411295
(20 rows)
```

The next query reports all the positive measurements made of all variables.

```
SELECT v.name, o.sequence, o.jd, f.name AS f, to_char (o.mag, '99D9999') AS mag, to_char (o.err, '0D9999') AS err, to_char (o.inst_mag, '99D9999') as i_mag, to_char(o.inst_err, '0D9999') AS i_err, o.reported AS rpt FROM variable v, observation o, filter f WHERE v.star=o.star AND o.filter=f.filter_id ORDER BY v.name;
         name         | sequence  |       jd       | f |   mag    |   err   |  i_mag   |  i_err  | rpt
----------------------+-----------+----------------+---+----------+---------+----------+---------+-----
 AL Com               | X25371ALM | 2458546.694832 | V |  19.0680 |  0.1488 |  21.8117 |  0.1482 | t
 CSS_J003149.5+415203 | X25366CE  | 2458817.423843 | V |  14.5748 |  0.0067 |  13.0930 |  0.0028 | f
 CSS_J003149.5+415203 | X25366CE  | 2458452.583906 | V |  14.5702 |  0.0115 |  16.5434 |  0.0104 | f
 CSS_J003149.5+415203 | X25366CE  |  2458840.41634 | V |  14.5369 |  0.0065 |  13.7170 |  0.0031 | f
 CSS_J003229.3+420354 | X25366CE  | 2458873.411961 | V |  16.9583 |  0.0365 |  17.7847 |  0.0362 | f
 CSS_J003229.3+420354 | X25366CE  | 2458457.480219 | V |  16.8283 |  0.0255 |  18.6265 |  0.0247 | f
 CSS_J003229.3+420354 | X25366CE  | 2458452.583906 | V |  16.8527 |  0.0642 |  18.8259 |  0.0640 | f
 CSS_J003229.3+420354 | X25366CE  |  2458840.41634 | V |  16.8645 |  0.0156 |  16.0446 |  0.0145 | f
 CSS_J003233.0+420013 | X25366CE  | 2458869.395041 | V |  13.6814 |  0.0077 |  13.8276 |  0.0037 | f
 CSS_J003233.0+420013 | X25366CE  |  2458840.41634 | V |  13.6983 |  0.0060 |  12.8784 |  0.0018 | f
 CSS_J003233.0+420013 | X25366CE  | 2458873.411961 | V |  13.7085 |  0.0064 |  14.5349 |  0.0040 | f
 CSS_J003233.0+420013 | X25366CE  | 2458817.423843 | V |  13.7261 |  0.0064 |  12.2443 |  0.0019 | f
 CSS_J003233.0+420013 | X25366CE  | 2458457.480219 | V |  13.7000 |  0.0066 |  15.4982 |  0.0021 | f
 CSS_J003233.0+420013 | X25366CE  | 2458452.583906 | V |  13.7177 |  0.0065 |  15.6909 |  0.0043 | f
 CSS_J003233.0+420013 | X25366CE  | 2458846.468642 | V |  13.6867 |  0.0078 |  13.6712 |  0.0008 | f
 DY Per               | X25371H   | 2458840.433308 | V |  13.2057 |  0.0031 |  12.3370 |  0.0029 | t
 DY Per               | X25371H   | 2458873.438068 | V |  12.3241 |  0.0024 |  12.4951 |  0.0022 | t
 DY Per               | X25371H   | 2458869.417772 | V |  12.4121 |  0.0041 |  12.4371 |  0.0038 | t
 DY Per               | X25371H   | 2458862.386765 | V |  12.5596 |  0.0123 |  14.1465 |  0.0102 | t
 DY Per               | X25371H   | 2458817.462158 | V |  13.9904 |  0.0030 |  12.8175 |  0.0029 | t
 DY Per               | X25371H   | 2458539.415692 | V |  11.1285 |  0.0024 |  14.0539 |  0.0011 | t
 DZ Per               | X25371H   | 2458869.417772 | V |  13.7774 |  0.0051 |  13.8024 |  0.0048 | f
 DZ Per               | X25371H   | 2458862.386765 | V |  13.8615 |  0.0214 |  15.4484 |  0.0203 | f
 DZ Per               | X25371H   | 2458840.433308 | V |  13.8934 |  0.0035 |  13.0247 |  0.0033 | f
 DZ Per               | X25371H   | 2458817.462158 | V |  13.8058 |  0.0026 |  12.6329 |  0.0025 | f
 DZ Per               | X25371H   | 2458539.415692 | V |  14.1160 |  0.0067 |  17.0414 |  0.0064 | f
 DZ Per               | X25371H   | 2458873.438068 | V |  13.9622 |  0.0047 |  14.1332 |  0.0046 | f
 GPX-TF8A-1104        | X25371H   | 2458869.417772 | V |  12.5230 |  0.0035 |  12.5480 |  0.0031 | f
 GPX-TF8A-1104        | X25371H   | 2458862.386765 | V |  12.5893 |  0.0126 |  14.1762 |  0.0105 | f
 GPX-TF8A-1104        | X25371H   | 2458840.433308 | V |  12.5683 |  0.0029 |  11.6996 |  0.0027 | f
 GPX-TF8A-1104        | X25371H   | 2458817.462158 | V |  12.4962 |  0.0017 |  11.3233 |  0.0015 | f
 GPX-TF8A-1104        | X25371H   | 2458539.415692 | V |  12.5699 |  0.0030 |  15.4953 |  0.0021 | f
 GPX-TF8A-1104        | X25371H   | 2458873.438068 | V |  12.4776 |  0.0025 |  12.6486 |  0.0023 | f
 MRK 421              | X25371ANS | 2458558.506611 | V |  13.3806 |  0.0067 |  16.6504 |  0.0042 | t
 V0742 Lyr            | X25371AOE |  2458736.42287 | V |  11.9379 |  0.0086 |  12.4576 |  0.0027 | t
(35 rows)
```

Note that LS And does not appear because it was too faint to be measured and AL Com was measurable (barely) only once on an especially deep image. Only observations of the five principal variables, those marked with 't' in the final column, have been reported to the BAAVSS photometry database

A crude measurement of the gain in productivity enabled by the software package is the ratio of all measurements of known variables to those submitted. The final pair of SQL queries give those values.

```
SELECT COUNT (v.star) FROM variable v, observation o WHERE v.star=o.star.
 count
-------
   35
(1 row)

SELECT COUNT (v.star) FROM variable v, observation o WHERE v.star=o.star AND o.reported='t';
 count
-------
    9
(1 row)
```

This estimate, 35/9 ≈ 4, is very crude because it does not take into account negative observations (as noted above, LS And falls into this category), nor does it indicate what may be found in the complete set of 11297 measurements. Nonetheless, it suggests that productivity has improved several-fold.

Conclusion:

My answer to the question posed in the title of this article is an unequivocal and enthusiastic YES!

Addendum:

All these scripts and the database schema are freely available on email request to the author at paul@leyland.vispa.com. It is only fair to point out that they are not yet a polished final product and users will be expected to investigate the internal workings in case of difficulty and to contact the author for assistance where necessary. The scripts (at present) have a dependency on a number of standard Perl modules, on a PostgreSQL database, on SWarp for image stacking, on the solve-field plate solving program from astronomy.net, and on APT for aperture photometry. There seems to be no reason why any of these dependencies cannot be changed, given a sufficient incentive to do so. To the best of my knowledge, all components should work unchanged on any Unix-like, Windows or MacOS operating system. If my knowledge is at fault I welcome re-education and especially so if it includes instructions on how to fix any deficiency detected in the software.

Acknowledgement:

I wish to thank Bert Pablo of the AAVSO for his assistance with programmatic access to the AAVSO's databases.

SAO 28567: One that got away

Christopher Lloyd

cl57@ymail.com

SAO 28567 was a suspected variable that was observed with the Ells Automatic Photometric Telescope in 1997. No variation was found at the time, but subsequent observations, most recently with TESS, have shown that it is a low amplitude ellipsoidal variable with a range of 0.^{m}019 that put it just out of reach of the APT.

Over the years there have been various efforts to confirm or otherwise the suspected variability of many stars. Some of these come with a long and painful history, while others occur spontaneously. One such suspect was SAO 28567, which is a bright, V = 6.78, star with a spectral type of A0 IV. It was noticed during visual observations of Comet C/1996 (Tabur) to be significantly brighter than shown in Uranometria, and in the SAO (7.9), PPM (7.6), and HD (7.9) catalogues (Poyner, 1996). Follow-up observations were made on 10 nights during the 1997 observing season using the Jack Ells Automatic Photometric Telescope (APT) (see Ells & Ells, 1989, 1990a,b) by members of the Crayford Manor House Astronomical Society (CMHAS) and reported by Pickard (1998) in the *Circular*. In total some 800 observations were made and from the stability of the comparison stars the internal errors were estimated at 0.^{m}03. Ultimately, no significant variation was found beyond the scatter of 0.^{m}04–5 in the data, so there was nothing to support the reported claim of variability, and no periodic signal was detected above a full amplitude of 0.^{m}01. However, it was noted with some agitation that there were,*'...discrepancies in the information given for this star in the various catalogues!,'* that unnecessarily led to it being a suspected variable. The mean magnitude from the APT of V = 6.75±0.03 was consistent with the Hipparcos and Tycho catalogue V_T magnitude.

Hipparcos did not provide a variability flag for this star, which actually meant that it was not possible to reliably determine if the star was variable or constant. However, that question was resolved, at least in part, by Koen & Eyer (2002) who found a period of 0.^{d}70670 in the *Hp* data, with a semi-amplitude of 0.^{m}008. Further ground-based photometry by De Cat et al. (2007) confirmed the variability, and as it showed a significant radial velocity variation, the star was most likely a close binary, so was classified as an ellipsoidal variable with twice the period. The Ells APT and Hipparcos data folded on the orbital period are shown in Fig. 1, and despite the noise there is a suggestion of the variation in the APT

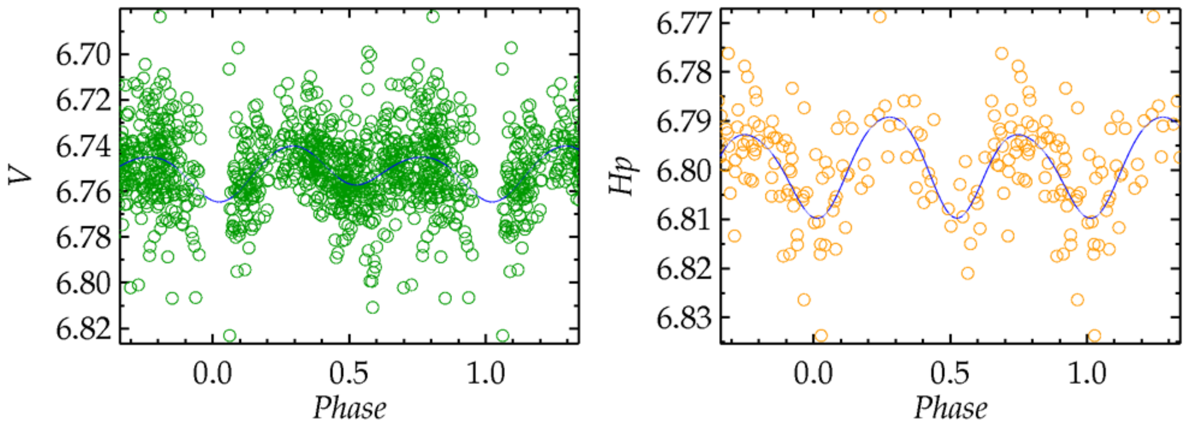

Figure 1: Phase plot of the clipped Ells APT V data (left) and the unflagged Hipparcos Hp data (right), folded on the orbital ephemeris in Equation 1. The lines are a low-order Fourier fits for illustration. The rms residual is 0.^{m}016 for the APT and 0.^{m}008 for the Hipparcos data.

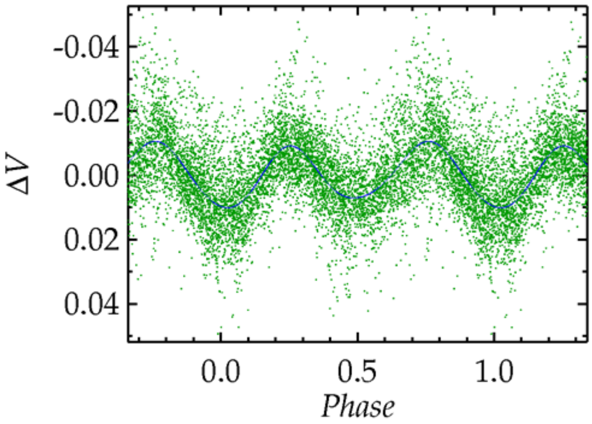

Figure 2: Phase plot of the clipped MASCARA *V* data, folded on the orbital ephemeris in Equation 1. The line is a low-order Fourier fit for illustration. The rms residual is $0.^{m}010$.

data. It turns out that one of the dominant frequencies found in the periodogram published by Pickard corresponded to an alias of the true half period, but a cluster of similar strength features around 18 c/d meant that there was no clearly identifiable period. Periods in the region of one day were, and still are, particularly challenging to investigate from the ground due to unresolved extinction effects, and the requirement to combine data from several nights to complete the light curve.

Part of the power of the APT came from its ability to use continuous coverage and weight of numbers to suppress the noise. A more modern take on this approach comes from the Multi-site All-Sky CAmeRA (MASCARA) project on based La Palma (Burggraaff et al., 2018). Their light curve from 2015-2016 contains over 6800 points with a rms of $0.^{m}010$ and is shown in Fig. 2.

Much more information is now available in the era of large ground-based and satellite surveys including *Gaia* and TESS. The first three TESS sectors were analysed by Prša et al. (2022) who found P = 1.4135516(9) d and eclipse depths of $0.^{m}020$ and $0.^{m}008$. TESS (Ricker et al., 2015) observed the system in Sectors 15, 16, 22, 48, 49, 75 and 76 and the data were downloaded from the MAST archive at the STScI. The SPOC pipeline light curve products were used and provided nearly 100 000 data points. The best *mean* ephemeris is given by a 4-harmonic Fourier fit as

$$\mathrm{BJD_{TDB}} = 2459614.9015(4) + 1.4135221(2) \times E \quad (1)$$

(where BJD is within a few seconds of HJD) but the light curve shows significant cycle to cycle variation in the amplitude that generates apparent scatter in the phase diagram, and unexpectedly large uncertainties in the ephemeris. These variations do not appear to be due to high-frequency pulsations but are more closely tied to the orbital period. The minima have mean depths of $0.^{m}019$ and $0.^{m}013$, and the maximum at $\phi = 0.75$ is $0.^{m}003$ fainter than the other. The phase diagram is shown in Fig. 3 where the individual sectors are shown in different colours.

The star is now listed in the AAVSO VSX under V352 UMa as an ellipsoidal variable, but with slightly less conviction in the GCVS. The *Gaia* DR3 data (Gaia Collaboration et al., 2023) confirm the period and amplitude of the variation, and additionally provide a distance d = 193 pc and a low extinction $A_V = A_G = 0.17$, leading to an absolute magnitude $M_G = 0.15$. The spectral type of A0 IV suggests that the dominant component is slightly evolved and the *Gaia* T_{eff} = 10 026K and colour, $G_{BP}-G_{RP} = 0.049$, are consistent. The *Gaia* EDR3-derived Bailer-Jones et al. (2021) distance is a marginally closer, but consistent 189±7 pc, so the star is a relatively nearby, early-type dwarf. The luminosity and colour place the star on the top edge of the main sequence as given by *Gaia* (cf. Fig. 6 in Gaia

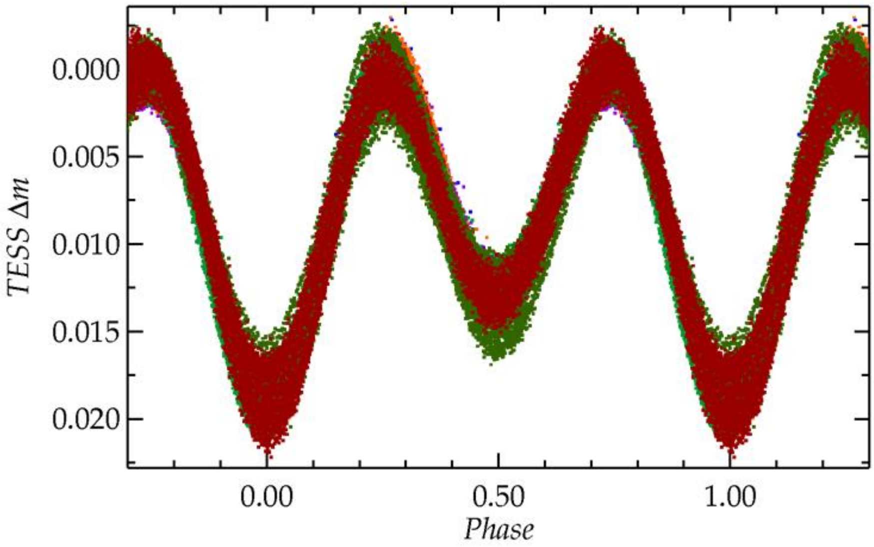

Figure 3: Phase diagram of the TESS data, using the ephemeris in Equation 1. The spread in the data is not noise, but coherent cycle to cycle variations. Most of the earlier data are obscured by the later high-cadence sectors.

Collaboration et al., 2018), but the influence of evolution or a companion is not clear. The velocity of the system is poorly constrained, but is most likely variable, so hopefully *Gaia* will provide an orbital solution relatively soon, and that will yield some information on the masses involved and the nature of the secondary.

Given that Hipparcos, at a cost of € 600 m, was working from space with photometric uncertainties of < 0.^{m}01, found it difficult to resolve the variability of this star, it is perhaps not too surprising that a home-made telescope on the outskirts of London, also failed, but it is equally miraculous that the APT came so tantalizingly close.

Enormous thanks to John Howarth for recovering the Ells APT photometry from a dusty archive, and to Malcolm Gough and the wider CMHAS team for supporting and maintaining the APT over the years. This paper includes data collected by the TESS mission, which are publicly available from the Mikulski Archive for Space Telescopes (MAST). Funding for the TESS mission is provided by NASA's Science Mission directorate.

References

Bailer-Jones, C. A. L., Rybizki, J., Fouesneau, M., et al., 2021, *AJ*, **161**, 147
Burggraaff, O., Talens, G. J. J., Spronck, J., et al., 2018, *A&A*, **617**, A32
De Cat, P., Briquet, M., Aerts, C., et al., 2007, *A&A*, **463**, 243
Ells, J. & Ells, P., 1989, *J BAA*, **99**, 282
Ells, J. & Ells, P., 1990a, *J BAA*, **100**, 24
Ells, J. & Ells, P., 1990b, *J BAA*, **100**, 30
Gaia Collaboration, Babusiaux, C., van Leeuwen, F., et al., 2018, *A&A*, **616**, A10
Gaia Collaboration, Vallenari, A., Brown, A. G. A., et al., 2023, *A&A*, **674**, A1
Koen, C. & Eyer, L., 2002, *MNRAS*, **331**, 45
Pickard, R., 1998, *VSS Circular*, **95**, 15
Poyner, G., 1996, *VSS Circular*, **90**, 3
Prša, A., Kochoska, A., Conroy, K. E., et al., 2022, *ApJ Suppl*, **258**, 16
Ricker, G. R., Winn, J. N., Vanderspek, R., et al., 2015, *Journal of Astronomical Telescopes, Instruments, and Systems*, **1**, 014003

Eclipsing Binary News

Des Loughney
desloughney@blueyonder.co.uk

MAST - Mikulski Archive for Space Telescopes

As it says on its website the MAST Portal lets you search multiple collections of astronomical datasets all in one place. I have been looking at the website to see what information is available on eclipsing binaries. I entered a search target which is one of our beginner systems, U Cephei, which has featured in VSSC articles. U Cephei was our Variable Star of the Year in 2006. The result of the search was 622 'hits' regarding photometry. In some of the 'hits' light curves are displayed. The screenshot below is an example of data that was obtained around about the 7th of December 2023. During the period covered by the data there are many examples of the primary eclipses from which the time of mid eclipse can be obtained. It should be possible to show whether the period of the system is changing (due to mass transfer) and by how much. I am looking forward to finding out how the times of mid eclipse (HJD) can be derived from TESS data.

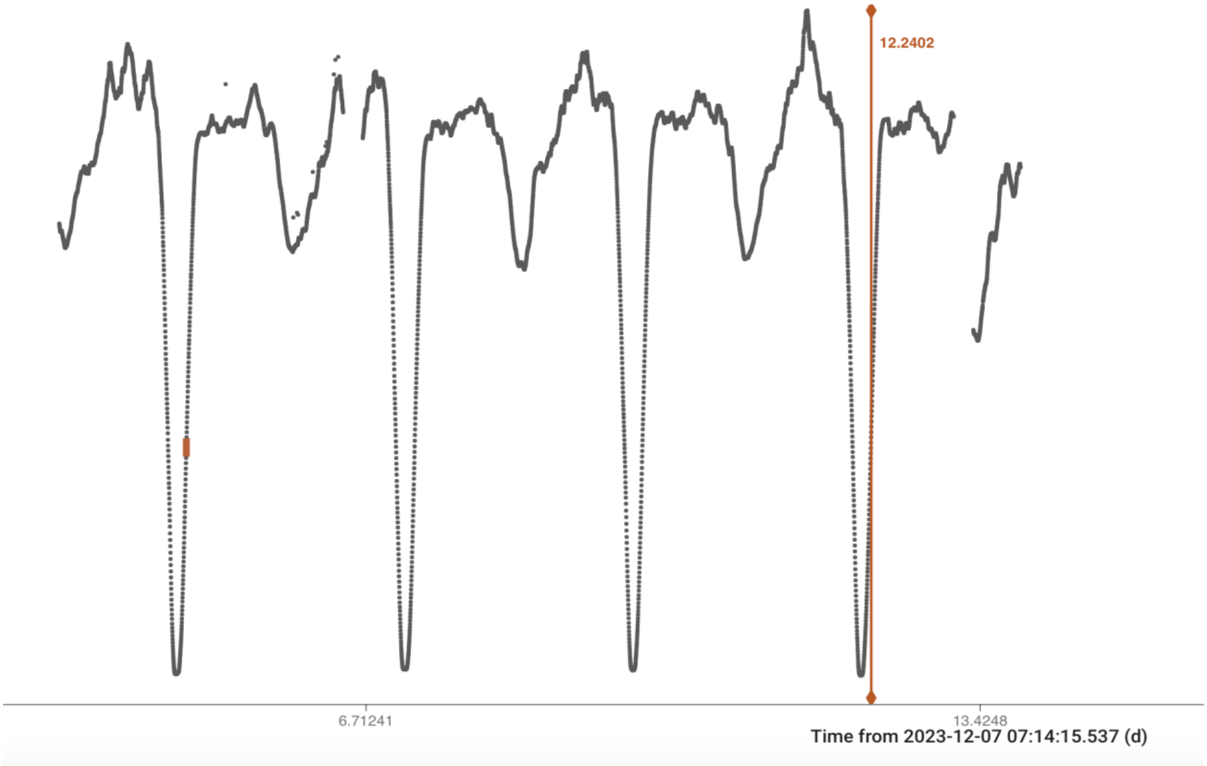

Eclipsing Binaries Exhibiting Period Changes

Mark Blackford can be seen on YouTube making a presentation on the above theme at a Variable Star South Symposium in 2022.

Modelling and Analysis of Eclipsing Binary Stars

This is a book by Andrej Prsa which was published in 2018 by the Institute of Physics. It can be downloaded from the IOP website as an e-book pdf file. It can also be purchased as a hard copy book. I hope to read it with interest and to be able to do a review for the next VSSC. In the meantime, the introductory blurb by the IOP reads:

"*The fascinating and observationally spectacular world of binary stars is a vast and beautiful one that is a significant aspect of many astrophysical studies. Modeling and Analysis of Eclipsing Binary Stars gives a comprehensive analysis and description of the science behind eclipsing binaries. It also explores the assumptions and the difficulties that can occur when using the modelling principles of the classical codes as well as introducing PHOEBE (the PHysics Of Eclipsing BinariEs)—a modern suite for modelling binary stars. PHOEBE was conceived by Andrej Prša and his collaborators and has become one of the standard tools in the eclipsing binary field*."

TIC 168789840: A Sextuply-Eclipsing Sextuple Star System [1]

In April 2024, the BBC Sky at Night Magazine reported on the above paper which dates to 2021. The system was discovered by analysing TESS data. The system is also known as TYC 7037-89-1. Using that as the target the data for the system can be viewed in MAST. As the paper states in the introduction TESS has dramatically improved our ability to discover multiple-star systems. There are over a hundred triple and quadruple candidates at present.

The Magazine has the diagram below which illustrates the system. There are three, A, B, and C, gravitationally bound eclipsing binaries.

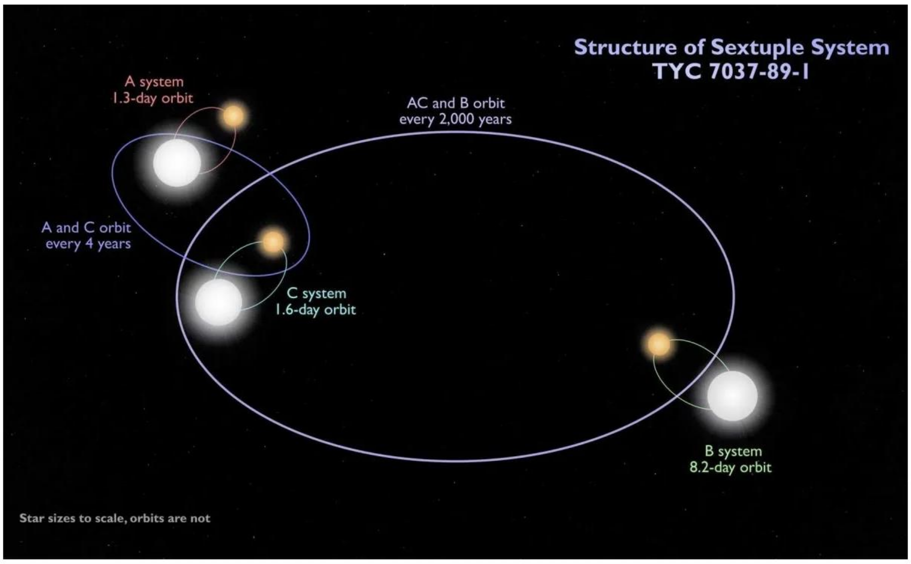

NASA infographic revealing the mechanics of the 6-star system of eclipsing binaries. Orbits shown are not to scale. Click to expand. Credit: NASA's Goddard Space Flight Center

The paper describes how ground-based measurements were necessary to refine the analysis of the system, and how the data supplied by TESS is improving. The early data was obtained at a 30-minute cadence but the latest data, used in the paper, was at a 2-minute cadence. Below is a figure from the paper which shows the type of light curve that is presented by the overlap of all the eclipses. The figure also shows the way the TESS data (blue) is combined with the model (red).

20

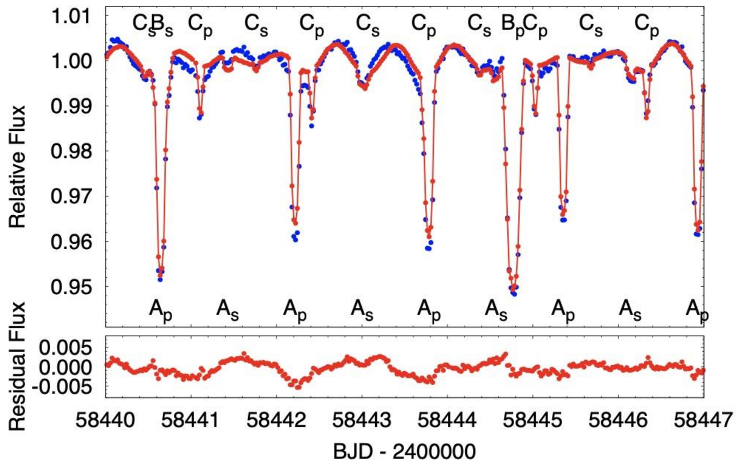

Figure 20. `Lightcurvefactory` photodynamical model for the overlapping set of eclipses superposed on a 7-day segment of the *TESS* data. Blue points are the data in 30-min cadence while the red curve is the model. The different EB eclipses are marked (e.g. A_p marks the primary eclipse of binary A).

References

1. TIC 168789840: A Sextuply-Eclipsing Sextuple Star System. Powell et al. https://arxiv.org/abs/2101.03433

V1177 Cassiopeiae: An unusual eclipsing binary

Christopher Lloyd and David Conner

cl57@ymail.com – david@somerbyconners.plus.com

The neglected, eccentric, long-period eclipsing binary V1177 Cas is shown to be a remarkable system. The eclipses are total with depths of $0^m.226$ and $0^m.174$ from TESS, but with very different FWHM of 0.0238 and 0.0078 in phase. The period has been refined to P=152.9415(9) and the system is eccentric with the secondary eclipse at ϕ_2 = 0.681(1). Both components are red giants with relative radii of about 2, but the separation at periastron means that some interaction between them is likely.

V1177 Cassiopeiae (GSC 04330-01963) is a neglected 11th magnitude long-period eclipsing binary, with eclipses about $0^m.3$ deep. Very little is known about the system and the VSX entry simply gives the type as EA and the period as 105 days, since corrected. It transpires that this value comes from the GCVS compilers (see the GCVS entry), so is not directly attributable, and they give no other details. Curiously, given its origin, a different period, *P* = 152.95d, is provided by Otero et al. (2006), and they also point to a displaced secondary indicating an eccentric system. As pointed out in the previous *Circular* by Conner (2024), this period is consistent with his data, while the GCVS period is not. The system is also included in a catalogue of eccentric binaries (Bulut & Demircan, 2007).

The study by Otero et al. (2006) is the only one of this system and pre-dates the 80th Name-List (Kazarovets et al., 2011) so it is not clear why their period was not reported. The data used by Otero et al. come from the Northern Variability Sky Survey (NSVS Woźniak et al., 2004), and are shown in Fig. 1. There are three apparent minima with separations of 153 and 104 days, and a gap, with a few faint points, which also falls at about 100–105 days after the first minimum. Otero et al. interpreted this as a period of 153d, with a significantly displaced secondary minimum. The GCVS period most likely comes from the 105-day spacing, but the reason for choosing it is not clear. The T_0 of the GCVS ephemeris is almost identical to that of Otero et al. and can only have come from the NSVS data.

In addition to the NSVS data V1177 Cas has been observed by the All-Sky Automated Survey for Supernovae (ASAS-SN) (Shappee et al., 2014, Kochanek et al., 2017) during 2015–2018 in *V* and from 2018 to the present in the Sloan *g*-band. Data are also available from the Zwicky Transient

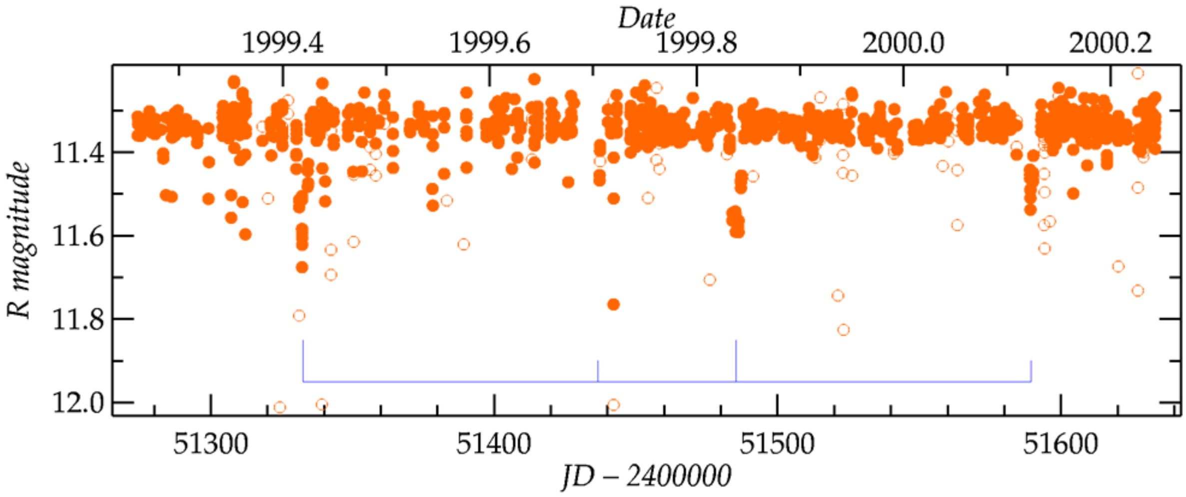

Figure 1: Epoch plot of the NSVS data, with the less reliable points indicated by open symbols. The ticks indicate the primary, and displaced secondary minima of the 153-day period.

Facility (ZTF) (Masci et al., 2019) from 2018 to the present in the Sloan *g*-band, although the star is a little bright for this instrument, and there is increased scatter for the brightest magnitudes, suggesting some non-linearity issues. Data are also available from the Kamogata/Kiso/Kyoto Wide-field Survey, which provides *V* and I_c data, but unfortunately these are too noisy to reliably identify the weak eclipses. As mentioned earlier, *V* -band data have been published by Conner (2024), covering the period from 2018 to the present. Finally, the star has been observed by TESS (Ricker et al., 2015) in Sectors 19 and 25, at the standard 30-minute cadence, Sector 52 at the 10-minute cadence, and Sectors 59 and 73 at the 200-second cadence. The Quick Look Pipeline (QLP) data were downloaded from the MAST archive at the STScI. Fortunately, TESS caught both eclipses. These were the primaries at JD $\simeq$ 2458826 (2019 December) and 2459744 (2022 June), but the first missed most of the egress and the second covered only part of the ingress, and one essentially complete secondary eclipse at JD $\simeq$ 2460307 (2023 December). All the other data were effectively constant. Even from the incomplete primary minimum it is clear that the eclipse is total, but this is not obvious for the secondary.

Due to the sparsity of the data in the eclipses, particularly the secondary, each data set has been analysed in its entirety. In an effort to quantify the properties of the light curves they have been modelled using the methodology described by Mikulášek (2015), which can fit a wide variety light of curve shapes using a small number of parameters. It is not a physical representation, but a mathematical parameterization of the light curve. The expression used is their Equation 14 in the full, double-eclipse form. The 'curvature' coefficient, C_k, is not necessary in this context and was set to zero. The higher-order K_k term was required to better fit the TESS data, but not used elsewhere. The parameters that can be determined directly from the fits are the central time, the zero level, that is the

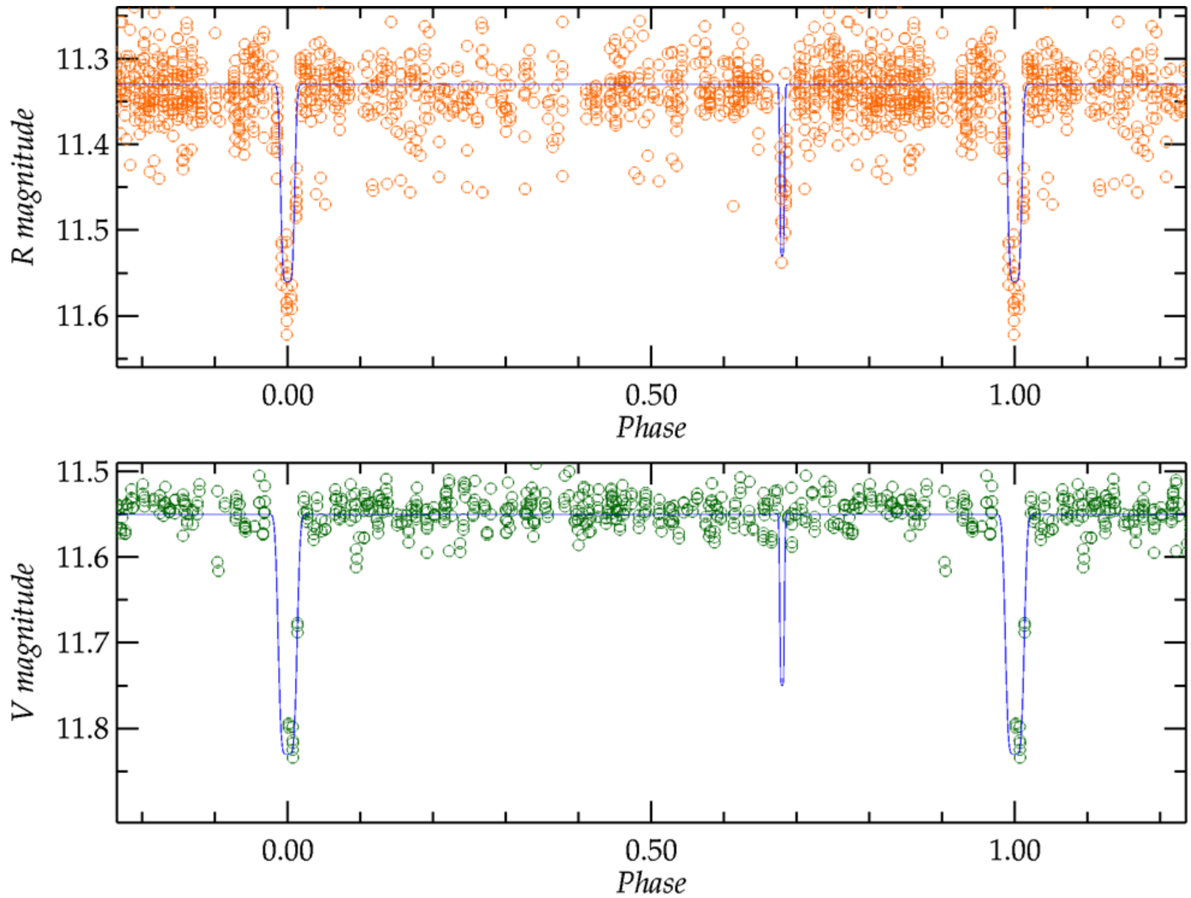

Figure 2: Phase diagrams of the different data sets, broadly in order of date, NSVS (top), ASAS-SN *V*. All panels are plotted to the same scale.

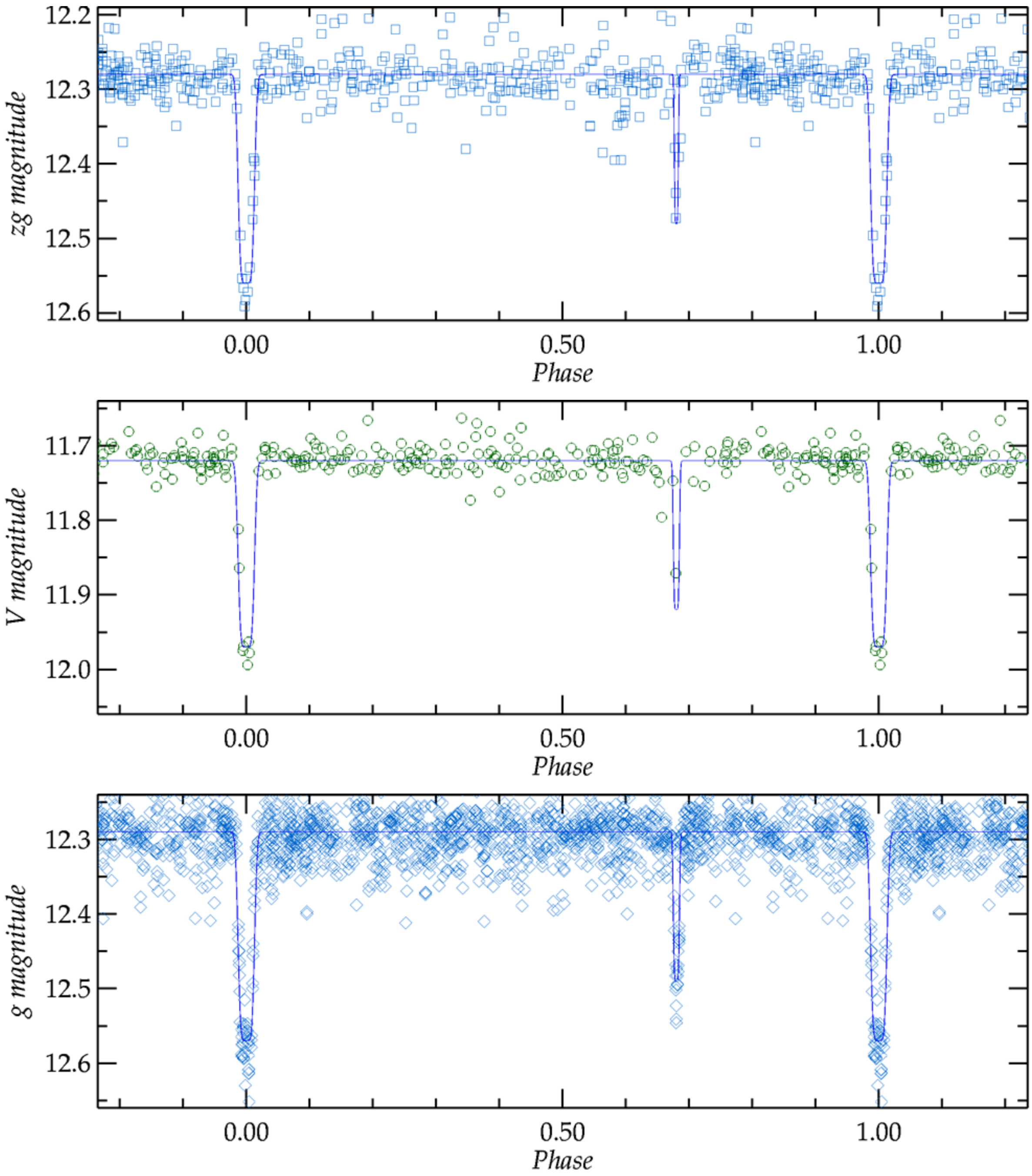

Figure 3: Phase diagrams of the different data sets, broadly in order of date, ASAS-SN *g*, ZTF *zg* and Conner's *V* data plotted to the same scale as Fig. 2.

out-of-eclipse magnitude, the depth of the minimum, and the full width. Less directly, it is also possible to measure the full width half maximum (FWHM) of the eclipse profile. In the initial fits most of the parameters were free unless they could not be sensibly determined from the data. The exception was the 'profile' parameter, Γ_k, which was fixed at the value derived from the TESS data, for both minima. An improved period was measured from these times of minima and then fixed in the final solutions. The fits to the individual data sets are shown in Fig. 2 for the NSVS and ASAS-SN *V* data, and Fig. 3 for the ASAS-SN *g*, ZTF data, and Conner's *V* data. The TESS data are shown in Fig. 4. For the ASAS-SN *V* data, the secondary eclipse fit shows the effect of the initial parameters, as the data were not sufficient to constrain the solution at this point.

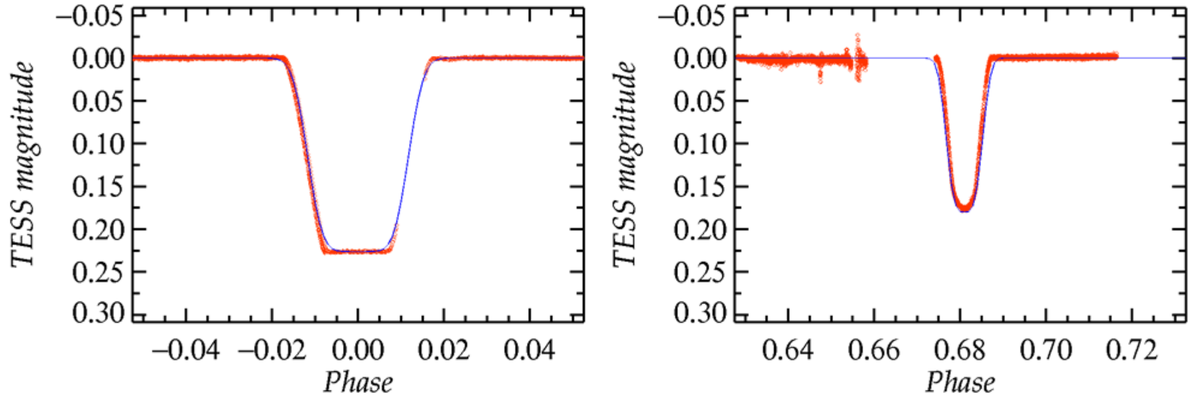

Figure 4: Phase diagram of the TESS data folded on the ephemeris. The primary eclipse (left) is based on one partial, and one very partial eclipse, while the secondary (right) is almost completely covered in one run. The points are shown in red, and the fit in blue. The constant data extend much further around the light curve.

Apart from the significant displacement of the secondary eclipse, the most obvious feature of the solutions is the difference in the widths of the eclipses. All the data sets show consistently that the secondary eclipse is much narrower than the primary by a factor of $\simeq 3$ and is a consequence of the elliptical orbit. TESS gives the FWHM of 0.02383(11) and 0.00781(2) in phase. The TESS data clearly show that the primary eclipse is total, and the density of points in the other data sets suggest that this may also be visible there. The best coverage comes from the ZTF and ASAS-SN *g* data, which give the primary depth as $0^m.28(1)$ and $0^m.284(5)$ respectively, and the sparse *V* data are similar at $0^m.26(1)$ and $0^m.27(1)$, while the NSVS are marginally shallower at $0^m.24(1)$. These compare to the very precise value from TESS of $0^m.226(1)$, and the difference is illustrated in the composite data shown in Fig 5. The TESS bandpass is a broad, unfiltered red, not unlike the NSVS, but certainly centred at a much longer wavelength than *V* or *g*, so the difference in depth may be an effective wavelength effect. If this is the case then it suggests that the star eclipsed at primary minimum is significantly hotter than the other component, which is the norm in eclipsing binaries. Given the lack of data the secondary eclipse is surprisingly well defined but is again dominated by the ASAS-SN *g* data. These give the depth as $\simeq 0^m.20$, again slightly deeper than the TESS value of $0^m.174(3)$. The

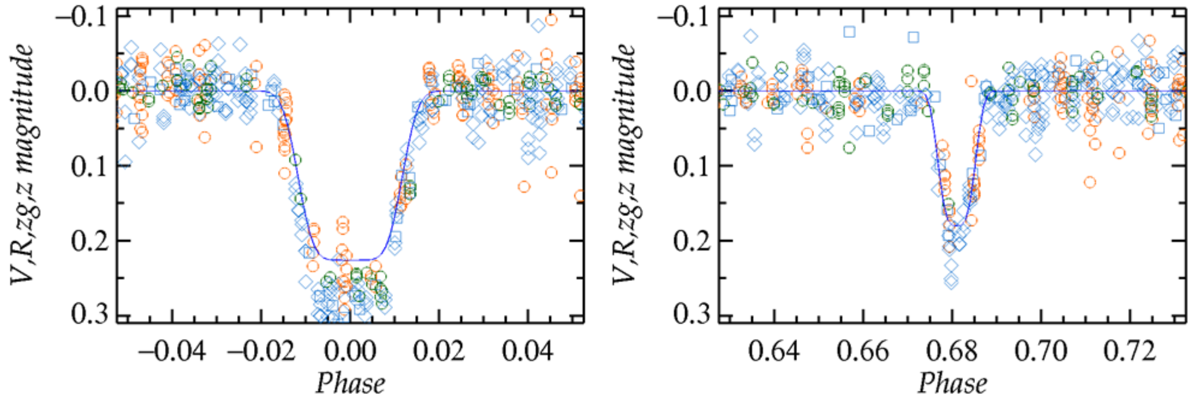

Figure 5: Phase diagram of the ground-based photometry. Composite plot of the relative magnitudes around primary minimum (left) and secondary minimum (right) of the NSVS, ASSN-SN, ZTF, and Conner's data, folded on the ephemeris. The line is the fit to the TESS data for both minima (cf. Fig. 4). The light curve is dominated by Sloan *g*-band data and the primary is noticeably deeper than the TESS eclipse, which suggests that the star being eclipsed is relatively blue, and less luminous than the other component. The secondary eclipse is also probably deeper at shorter wavelengths. Despite the weakness of the secondary eclipse the difference in the widths of the eclipses is obvious. The symbols are as before.

shape of the eclipse is not obviously total and given the elliptical orbit it is possible that with the right inclination one eclipse could be total and the other partial, which would affect the secondary depth and width. However, the shapes are typical of a smaller, hotter component being occulted at primary minimum, with a transit at secondary minimum, where limb darkening has a significant impact throughout the eclipse.

Times of minima have been taken from the fits to the individual data sets as possible, and each of these inevitably covers a large span of time. In addition, times have been measured using the Kwee & van Woerden (1956) (KvW) method for the best TESS primary minimum and the secondary. The primary measurement involves a large range of interpolated values through the egress, but the light curve fit from earlier is equally compromised by the lack of data. These values differ by much more than the combined errors, highlighting the uncertainty, but the secondary measurements are entirely consistent. The times of the eclipses have been used to derive a more reliable value for the period, and an unweighted fit gives a linear ephemeris of

$$HJD_{\text{MinI}} = 2451485.439(44) + 152.9415(9) \times E \qquad (1)$$

The process also optimized the phase of the secondary minimum to $\phi_2 = 0.681 \pm 0.001$. The residuals are shown in the O–C diagram in Fig. 6.

Assuming that both eclipses are total then it is possible to draw some conclusions about the components. Using the TESS eclipse depths of $0^m.226$ and $0^m.174$ immediately gives a magnitude difference of $1^m.82$ between the two components and the relative contribution 81% and 19% of the combined light in the red. Using the Sloan *g* eclipse depths leads to a slightly lower $\Delta g = 1^m.61$. The *Gaia* DR3 catalogue (Gaia Collaboration et al., 2023) gives $G = 11.114$, $G_{BP} = 11.915$, $G_{RP} = 10.238$, and $G_{BP} - G_{RP} = 1.678$.

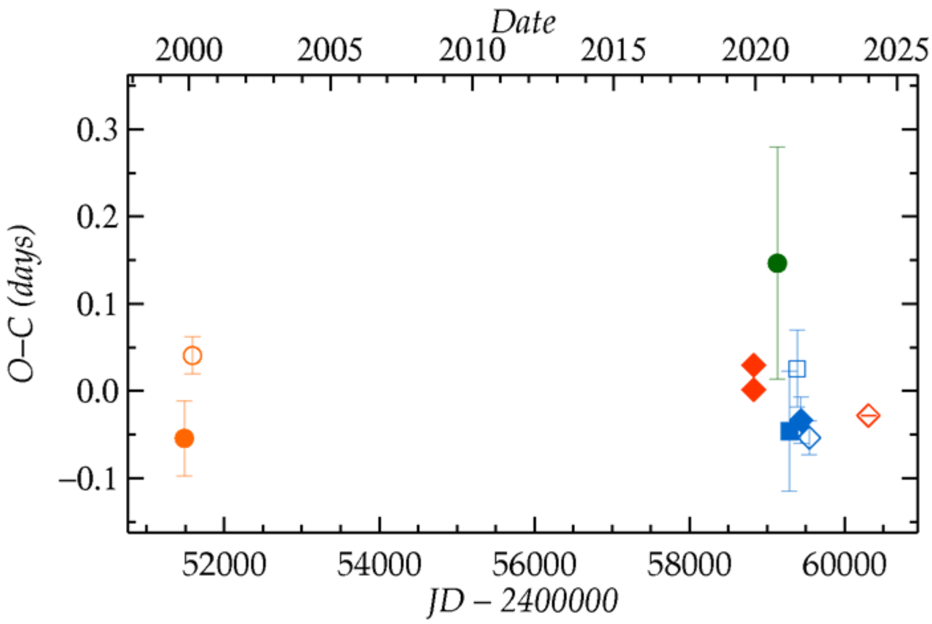

Figure 6: O–C diagram of the timing data given in Table 1 constructed using the ephemeris in Equation 1. The residual for the ASAS-SN *V* data lies off the top of the plot and is discounted as only part of the eclipse was covered. The TESS primary timings from the fit and KvW method are strictly inconsistent with each other, but are in good agreement with the other timings, while the TESS secondary is arguably the most reliable.

Table 1: Times of minima from the fits to each data set

HJD	σ	Min.	Cycle	O–C	Band	Data
2451485.3785	0.0428	1	0.00	−0.054	*R*	NSVS
2451589.6266	0.0213	2	0.68	+0.041	*R*	NSVS
2458826.6265	0.0021	1	48.00	+0.001	*C*	TESS (KvW)
2458826.6545	0.0019	1	48.00	+0.029	*C*	TESS
2459132.6545	0.1331	1	50.00	+0.146	*V*	Conner
2459285.4036	0.0688	1	51.00	−0.046	*zg*	ZTF
2459389.6284	0.0440	2	51.68	+0.026	*zg*	ZTF
2459438.3576	0.0266	1	52.00	−0.033	*g*	ASAS-SN
2459542.4906	0.0191	2	52.68	−0.054	*g*	ASAS-SN
2460307.2235	0.0006	2	57.68	−0.028	*C*	TESS
2460307.2237	0.0003	2	57.68	−0.028	*C*	TESS (KvW)

The distance from Bailer-Jones et al. (2021) is d = 860±13pc, which combined with the *Gaia* extinction A_G = 1.134, leads to an absolute magnitude of M_G = 0.3. Using the red relative contributions this resolves the individual absolute magnitudes to M_G = 0.5 and 2.3. Assuming that the secondary eclipse is not affected by the eccentricity of the system so is also total, then it is possible to estimate the relative radii of the cooler and hotter components as R_c/R_h = 2.3 and similarly for the relative temperatures as T_c/T_h = 0.94. *Gaia* gives a composite T_{eff} = 4800K, consistent with the colour of the system, so the effective temperatures are $T_c \simeq$ 4800K and $T_h \simeq$ 5100K. It appears that both components are evolved, red-giant-branch stars with relatively similar temperatures, but the cooler component has a radius of over twice the other star. The luminosity and temperature place the dominant component near the red-giant clump, while the other star is only slightly bluer, but $\simeq 1^m.8$ further down the giant branch (cf. Fig. 10 in Gaia Collaboration et al., 2018).

V1177 Cas is sufficiently bright that *Gaia* was able to obtain spectra and has determined a single-lined spectroscopic binary orbit from 24 velocities. The period, P = 153.14±0.12d is consistent with the value determined here, but less precise, and the other elements are e = 0.555±0.011, ω = 118.4±1.1°, and K = 33.6±0.4kms^{-1}. The quantity $e \cos \omega = -0.26$ calculated directly from the spectroscopic elements is consistent with the approximate equality $e \cos \omega \simeq \pi/2(1/2 - \phi_2) = -0.28$ from the photometric solution (Charbonneau et al., 2005, Hilditch, 2001).

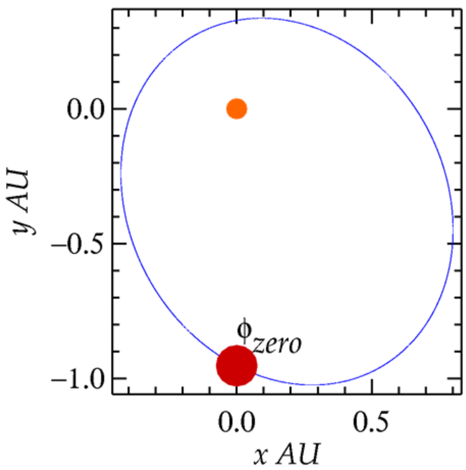

Figure 7: Projection of the spectroscopic orbit of the more luminous component onto a plane normal to the sky. The observer is in the -y direction and the eclipses occur at x =0. The scale of the plot is set by the assumption that the total mass of the system is $2M_\odot$, which gives a = 0.705AU or $152R_\odot$. The primary component is assumed to have $r = 15R_\odot$ and both components are plotted to scale.

Most red giants have masses in the 1–1.5$M_\odot$ range (Hekker et al., 2011), so assuming a total mass for the system of a conservative 2$M_\odot$ it is possible to calculate the semi-major axis a = 0.705AU or 152$R_\odot$. The radii of red giants cover a very wide range, but for those near the red-giant clump $r \simeq$ 10$R_\odot$ (Hekker et al.), and for less evolved early K-type giants, values of 15–30$R_\odot$ are more likely (Dyck et al., 1996). At periastron the separation of the two components is 48$R_\odot$, which could be just twice the combined radii, so there is very likely some periodic interaction between them. Obviously, if the stars are more massive than assumed then the system will be larger. The orbit is plotted to scale in Fig. 7 and is consistent with the interpretation of the light curve. At secondary minimum the components are separated by about a third of the distance at primary minimum, so the components are about three times larger in their respective skies and might be expected to produce eclipses about three times longer. However, the duration of the eclipses is also dependent on the speed at which the components move, and in this case, there is a factor of about 12 in the angular velocity between periastron and apastron, which accounts for the narrowness of the secondary eclipse.

The system most probably contains two evolved stars that are both making their way up the giant branch for the first time. Given the eccentricity of the system there has probably been little interaction between them so far, but with the increasing radii and the small separation at periastron, that may already be changing.

The authors would like to thank Klaus Bernhard for helpful input. This paper includes data collected by the TESS mission, which are publicly available from the Mikulski Archive for Space Telescopes (MAST). Funding for the TESS mission is provided by NASA's Science Mission directorate.

References

Bailer-Jones, C. A. L., Rybizki, J., Fouesneau, M., et al., 2021, *AJ*, **161**, 147
Bulut, I. & Demircan, O., 2007, *MNRAS*, **378**, 179
Charbonneau, D., Allen, L. E., Megeath, S. T., et al., 2005, *ApJ*, **626**, 523
Conner, D., 2024, *VSS Circular*, **200**, 59
Dyck, H. M., Benson, J. A., van Belle, G. T., et al., 1996, *AJ*, **111**, 1705
Gaia Collaboration, Babusiaux, C., van Leeuwen, F., et al., 2018, *A&A*, **616**, A10
Gaia Collaboration, Vallenari, A., Brown, A. G. A., et al., 2023, *A&A*, **674**, A1
Hekker, S., Gilliland, R. L., Elsworth, Y., et al., 2011, *MNRAS*, **414**, 2594
Hilditch, R. W., 2001, *An Introduction to Close Binary Stars*, Cambridge University Press
Kazarovets, E. V., Samus, N. N., Durlevich, O. V., et al., 2011, *IBVS*, **5969**, 1
Kochanek, C. S., Shappee, B. J., Stanek, K. Z., et al., 2017, *PASP*, **129**, 104502
Kwee, K. K. & van Woerden, H., 1956, *Bulletin of the Astronomical Institutes of the Netherlands*, **12**, 327
Masci, F. J., Laher, R. R., Rusholme, B., et al., 2019, *PASP*, **131**, 018003
Mikulášek, Z., 2015, *A&A*, **584**, A8
Otero, S. A., Wils, P., Hoogeveen, G., et al., 2006, *IBVS*, **5681**, 1
Ricker, G. R., Winn, J. N., Vanderspek, R., et al., 2015, *Journal of Astronomical Telescopes, Instruments, and Systems*, **1**, 014003
Shappee, B. J., Prieto, J. L., Grupe, D., et al., 2014, *ApJ*, **788**, 48
Woźniak, P. R., Vestrand, W. T., Akerlof, C. W., et al., 2004, *AJ*, **127**, 2436

Section Publications

Hard Copy Charts	Order From	Charge
Telescopic	Chart Secretary	Free
Binocular	Chart Secretary	Free
Eclipsing Binary	Chart Secretary	Free
Observation Report Forms	Director/Red Star Co-ordinator	Free
Chart Catalogue	Director	Free
Binocular VS charts Vol 2	Director or BAA Office	Free

Charts for all stars on the BAAVSS observing programmes are freely available to download from the VSS Website www.britastro.org/vss

Contributing to the VSS Circular

Written articles on any aspect of variable star research, observing or letters are welcomed for publication in these circulars. The article must be your own work and should not have appeared in any other publication. Acknowledgement for light curves, images and extracts of text must be included in your submission if they are not your own work! References should be applied where necessary. Authors are asked to include a short abstract of their work when submitting to these circulars.

Please make sure of your spelling before submitting to the editor. English (not US English) is used throughout this publication.

Articles can be submitted to the editor as text, RTF or MS Word formats. Light curves, images etc. may be submitted in any of the popular formats. Please make the font size for X & Y axes on light curves large enough to be easily read.

Email addresses will be included in each article unless the author specifically requests otherwise.

Deadlines for contributions are the 15th of the month preceding the month of publication. Contributions received after this date may be held over for future circulars. Circulars will be available for download from the BAAVSS web pages on the 1st day of March, June, September and December.

Deadline for the next VSSC is November 15th 2024.

BAA www.britastro.org
BAAVSS www.britastro.org/vss
BAAVSS Database https://www.britastro.org/photdb/
BAA Spectroscopic Database https://britastro.org/specdb/
BAAVSS *Circular* Archive http://www.britastro.org/vss/VSSC_archive.htm

Back to contents

Section Officers

Director
Prof. Jeremy Shears
Pemberton, School Lane, Tarporley, Cheshire CW6 9NR
Tel: 07795 223869 E-mail bunburyobservatory@hotmail.com

Secretary
Bob C. Dryden
21 Cross Road, Cholsey, Oxon OX10 9PE
Tel: 01491 201620 E-mail visual.variables@britastro.org

Chart Secretary
John Toone
Hillside View, 17 Ashdale Road, Cressage, Shrewsbury SY5 6DT
Tel: 01952 510794 E-mail enootnhoj@btinternet.com

Pulsating Stars Co-ordinator
Shaun Albrighton
4 Walnut Close, Hartshill, Nuneaton, Warwickshire CV10 0XH
Tel: 02476 397183 E-mail shaunalbrighton93@gmail.com

CV's & Eruptive Stars Co-ordinator, *Circular*s Editor & Webmaster
Gary Poyner
67 Ellerton Road, Kingstanding, Birmingham B44 0QE
Tel: 07876 077855 E-mail garypoyner@gmail.com

Nova/Supernova Secretary
Guy Hurst
16 Westminster Close, Basingstoke, Hants RG22 4PP
Tel: 01256 471074 E-mail guy@tahq.org.uk

Eclipsing Binary Secretary
Des Loughney
113 Kingsknowe Road North, Edinburgh EH14 2DQ
Tel: 0131 477 0817 E-mail desloughney@blueyonder.co.uk

Database Secretary
Andy Wilson

Tel: 01934 830683 E-mail andyjwilson_uk@hotmail.com

Telephone Alert Numbers for Nova and Supernova discoveries telephone Denis Buczynski 01862 871187. Variable Star alerts call Gary Poyner or post to BAAVSS-Alert – **but please make sure that the alert hasn't already been reported**.

Back to contents